

USE OF METAL ALLOYS FOR  
ADIABATIC DEMAGNETIZATION

by

David Torrison Nelson

A Dissertation Submitted to the  
Graduate Faculty in Partial Fulfillment of  
The Requirements for the Degree of  
DOCTOR OF PHILOSOPHY

Major Subject: Physics

Approved:

Signature was redacted for privacy.

In Charge of Major Work

Signature was redacted for privacy.

Head of Major Department

Signature was redacted for privacy.

Dean of Graduate College

Iowa State University  
Of Science and Technology  
Ames, Iowa

1960

## TABLE OF CONTENTS

	Page
INTRODUCTION	1
BASIC CONCEPTS	15
Thermodynamics of Adiabatic Demagnetization	15
Magnetic Fields in Material Media	17
Normal Paramagnetism	18
Ferromagnetism and Antiferromagnetism	20
MATERIALS TESTED	22
Preparation	22
Single Crystals	23
Purity	23
EXPERIMENTAL PROCEDURE	29
Magnetic Susceptibility Measurements	29
Magnetization Measurements	41
Adiabatic Demagnetization Measurements	46
RESULTS	50
Susceptibility Measurements	50
Magnetization Measurements	59
Adiabatic Demagnetization Measurements	73
DISCUSSION	82
SUMMARY	94
LITERATURE CITED	96
ACKNOWLEDGMENTS	100

## INTRODUCTION

In order to study fundamental interactions in matter on a macroscopic scale it is necessary that the interaction energy be of the order of magnitude of the thermal energy associated with the temperature of the material. In general, interaction energies cover a wide range for various physical phenomena. Thus the extent to which it is necessary to lower the temperature to study a particular phenomenon depends on the weakness of the interaction. In the case of magnetism some metals are ferromagnetic at room temperature whereas others do not become ferromagnetic until cooled to the liquid helium region of temperature. To study superconductivity it is necessary to work at temperatures below 20 °K and usually below 4 °K. In order to study nuclear orientation it is often necessary to work at temperatures in the neighborhood of 0.001 °K. It is understandable then that the attainment of temperatures below 1 °K has been one of the major efforts in low temperature research during the past thirty years or so.

The field of low temperature research was opened in 1908 with the liquefaction of helium by Kammerlingh Onnes (1). Liquid helium boils under atmospheric pressure at 4.2 °K, and the boiling temperature can be lowered by reducing the pressure over the liquid. In 1932 Keesom (2) achieved a bath temperature reported as 0.71 °K but only by using tremendous diffusion pumps with a pumping speed of 675 liters per second. A similar bath temperature was obtained by Blaisse et al. (3) who reduced the heat loss up the superfluid liquid He II film by applying a narrow

constriction in the helium dewar. By this means they needed a pumping speed of only 10 liters per second. However this appeared to be the lower limit of temperature obtainable by pumping on a bath of liquid helium. Ordinarily in the laboratory 1.0 °K represents the practical lower limit of temperature obtainable in this way.

A method for obtaining temperatures below 1 °K by the adiabatic demagnetization of a paramagnetic salt was proposed in 1926 independently by Debye (4) and Giauque (5). In 1933 the first experimental results of adiabatic demagnetization of a paramagnetic salt were given by Giauque and McDougall (6) in which a lowest temperature of 0.25 °K was reported. Almost simultaneously reports from deHaas et al. (7) and Kurti and Simon (8) indicated success in achieving temperatures well below 1 °K. This method has subsequently been developed so that it has become a standard procedure for obtaining very low temperatures.

The lowest temperature that can be attained with this method is roughly that for which  $kT$  is of the order of the interaction energy between magnetic ions. Although this temperature can be lowered by diluting the magnetic ions in the salt with the addition of nonmagnetic ions, such a process also decreases the entropy which can be extracted from the salt. In the limit of extreme dilution the dominant contribution to the entropy at 1 °K would be that of the lattice. As pointed out by Ambler and Hudson (9) 0.001 °K is probably the lower limit of temperature attainable by demagnetization of a paramagnetic salt.

Although a paramagnetic salt can be cooled below 1 °K rather easily,

it is not a particularly simple task to cool other materials by contact with a salt. As shown by Kurti et al. (10) the thermal conductivity of a paramagnetic salt is very low at these temperatures, making thermal contact with a specimen very difficult to achieve. They found that the approach to thermal equilibrium of a single crystal of chromium potassium alum whose ends were at different temperatures was too short to be measured above 0.3 °K and too long to be measured below 0.14 °K. Various schemes have been tried for making thermal contact between a sample and a cooling salt. Some of the more successful methods are a copper vane technique described by Mendoza and Thomas (11) in which powdered salt is pressed into a copper vane assembly. The sample then is put into thermal contact with the copper. Meyer (12) describes a method whereby a single crystal of a paramagnetic salt is put into thermal contact with the sample with many strips of silver ribbon glued between the sample and salt crystal. Quite recently Miedema et al. (13) have studied heat transfer through solid alcohol solutions of paramagnetic salts. Thermal contact between the solid solution and a sample is achieved through many copper wires which are attached to the sample at one end and buried in the solid solution at the other. The difficulty of poor thermal conduction is enhanced by the fact that there is a continuous heat leak from the surroundings to the specimen and salt pill which may spoil the temperature homogeneity between them.

In 1949 Daunt and Heer (14) proposed a technique for the establishment of continuous refrigeration at temperatures well below 1 °K. Heer

et al. (15) announced in 1953 the successful operation of the first magnetic refrigerator. The device employed a cyclic adiabatic demagnetization-isothermal magnetization process for maintaining a constant temperature bath to temperatures as low as 0.3 °K. In further experiments Heer et al. (16) were able to reach and maintain a temperature of 0.2 °K. They showed that the theoretical limit at which heat extraction equaled heat input was 0.1 to 0.15 °K. However, they suggested that temperatures as low as 0.05 °K could be maintained with a two engine unit.

Mendelssohn and Moore (17) performed experiments in 1934 on the adiabatic magnetization of superconducting tin. They showed that a cooling of 0.33° occurred at 2.5 °K by magnetizing with a field considerably higher than the threshold value. They suggested the method as a simple means of producing very low temperatures. In 1936 Mendelssohn et al. (18) achieved a temperature estimated to be between 0.2 and 0.3 °K by this method. Mendelssohn (19) has pointed out that temperatures well below 0.1 °K could be obtained by using metals such as tantalum and niobium which have high critical temperatures. He suggested, however, that this method could be best put to use in the temperature range 0.3 to 1.0 °K. The specific heat of a metal increases linearly with temperature so that, as the temperature of the specimen rises, the heat influx is balanced by a steadily increasing heat capacity, retarding the warmup rate. Below 0.3 °K the specific heat of a metal is small in comparison to that of paramagnetic salts, so that a salt is a more effective coolant in this temperature region.

Following experiments in 1939 by Daunt and Mendelssohn (20), Kapitza (21) in 1941 concluded that appreciable drops in temperature might be obtained from a process based on the mechanocaloric effect in liquid helium II. On the two fluid model of liquid helium II, the normal fluid has a nonzero viscosity and a nonzero entropy whereas the superfluid component is a superfluid and has zero entropy (22). Consequently if liquid helium II is passed through a narrow tube (about  $10^{-3}$  mm diameter) a separation of the phases will occur with a consequent heating at the entrance and cooling at the exit of the tube. Simon (23) has shown that the method would be very inefficient, however, due to the fact that liquid helium has lost almost all its entropy at temperatures not much below 1 °K. It is thus almost devoid of cooling power at very low temperatures.

Sydoriak et al. (24) in 1948 succeeded in liquefying  $\text{He}^3$  and found that liquid  $\text{He}^3$  has a considerably higher vapor pressure than liquid  $\text{He}^4$  at a given temperature. Zinov'eva (25) employed this fact in experiments on the surface tension of liquid  $\text{He}^3$  in order to extend his measurements to 0.35 °K by pumping away the vapor from over the liquid. Sydoriak and Roberts (26) have measured the vapor pressure of liquid  $\text{He}^3$  and established the vapor pressure-temperature relation down to 0.3 °K. Seidel and Keesom (27) have developed a  $\text{He}^3$  cryostat for use in calorimetric measurements down to 0.3 °K. With the increased availability of  $\text{He}^3$  gas this method for production of temperatures in the range 0.3 - 1.0 °K is gaining wide application.

In 1953 Sommers et al. (28) demonstrated the heat of mixing of  $\text{He}^3$

in  $\text{He}^4$  by adiabatically mixing the two liquids and observing the drop in temperature. They showed the heat of mixing for an 8.6 percent solution of  $\text{He}^3$  in  $\text{He}^4$  at 1.0 °K to be 0.17 calorie per mole of solution. This resulted in a cooling of the mixture from 1.0 °K to 0.78 °K. Quite recently London as quoted by Brewer (29) has analyzed the possibility of using the reversible adiabatic dilution of liquid  $\text{He}^3$  with liquid  $\text{He}^4$  in order to obtain temperatures below 1 °K. He suggested that reversible dilution could be achieved by introducing superfluid  $\text{He}^4$  through a superleak into pure liquid  $\text{He}^3$  or into a  $\text{He}^3$  -  $\text{He}^4$  mixture.

In order to obtain temperatures below 0.001 °K it was suggested independently by Gorter (30) and Kurti and Simon (31) that nuclear paramagnetism be used in magnetic cooling. Since nuclear magnetic moments are about a thousand times smaller than electronic magnetic moments, such a cooling process, to be effective, must have a starting temperature near 0.01 °K and an initial magnetic field of the order of 100 koe. Rollin and Hatton (32) in 1948 were the first to obtain cooling by this method. Working with a fluorine salt they lowered the temperature of the nuclear spin system to 0.17 °K from starting conditions of 1.2 °K and 4 koe. The spin temperature was observed to rise back to the lattice temperature of 1.2 °K with a relaxation time of 60 sec. No appreciable cooling of the lattice was effected because of the extremely small amount ( $10^{-4}$  percent) of entropy removed compared to the total entropy at 1.2 °K.

Experiments by Kurti et al. (33) in 1956 were successful in cooling the nuclear spin system of copper metal to about  $20 \times 10^{-6}$  °K although they were uncertain as to whether the lattice and electrons were also



cooled to this temperature. In more recent experiments of Hobden and Kurti (34) a spin temperature for copper nuclei of  $1.2 \times 10^{-6}$  °K was achieved; however the observed relaxation time indicated that the lattice and conduction electrons did not participate in the cooling.

In summary it can be seen that temperatures well below 1 °K have been obtained. For temperatures to 0.3 °K the He<sup>3</sup> cryostat now seems the most practical method. The magnetic refrigerator has the advantage over a He<sup>3</sup> cryostat of maintaining a heat bath down to the lower temperature of 0.2 °K. Below these temperatures and down to 0.001 °K the adiabatic demagnetization of a paramagnetic salt has been found to be the only practical method.

As pointed out above, there are serious difficulties in obtaining thermal contact between a paramagnetic salt and a sample cooled by it when the temperature is below about 0.1 °K. The present research was undertaken with the view in mind of finding a metal alloy which could be used to produce cooling by adiabatic demagnetization. In order to be effective, such an alloy would need to be dilute enough to retain a large fraction of its electronic thermal conductivity, and yet contain enough magnetic ions so that a sufficient entropy could be extracted during the magnetization at 1 °K. Also the magnetic transition temperature of the alloy should be near the temperature to be obtained by adiabatic demagnetization, so that there would be a peak in the specific heat at this point.

There are some low temperature experimental data available at present on magnetic properties of dilute alloys of transition metals

dissolved in a noble metal. Owen et al. (35) have reported susceptibility measurements on dilute alloys of manganese dissolved in copper. They found that the Curie temperature was a strong function of the manganese concentration being 7 °K for 1.4 atomic percent manganese and 100 °K for 11.1 atomic percent manganese. Further, they found the susceptibility to be only about 75 percent of its value expected on the basis of the free doubly positive manganese ion. Hedgcock (36) reported susceptibility measurements on single crystals of very dilute alloys of iron in copper. He found that a 0.016 atomic percent iron in copper alloy was weakly paramagnetic down to the lowest observed temperature of 4.2 °K. Experiments of Schmitt and Jacobs (37) on dilute alloys of manganese in copper showed that magnetic remanence occurred at 1.76 °K with as little as 0.4 atomic percent manganese. No remanence was observed for manganese concentrations of 0.2 and 0.05 percent down to 1.8 °K which was the lowest temperature investigated. Jacobs and Schmitt (38) have reported further experiments on dilute alloys of manganese in copper for which the magnitude of the remanence was measured. They also measured the susceptibility of three alloys of cobalt in copper with 0.5, 1.0, and 2.0 atomic percent cobalt. The results of these latter measurements showed that a Curie-Weiss law for susceptibility versus temperature did not hold in the temperature range of measurement.

Very few magnetic data are available on dilute alloys of rare earth metals in a nonmagnetic matrix. Bates and Newmann (39) have made susceptibility measurements on alloys of cerium in thorium and found a well defined minimum in the plot of inverse susceptibility versus temperature for all samples tested. The cerium concentration ranged

from 5 atomic percent to 90 atomic percent, and the temperature of the susceptibility maximum was highest for the 5 percent sample, being close to 300 °K.

Matthias et al. (40) have investigated alloys of rare earths in lanthanum in order to determine the dependence of the superconducting transition of lanthanum on the spin of the solute. In the course of their investigation they found that gadolinium-lanthanum alloys with more than 3.0 atomic percent gadolinium were ferromagnetic. The ferromagnetic Curie temperature varied almost linearly from 1.3 °K at 3.0 percent to 6.0 °K at 10.0 percent gadolinium. They also reported that only moderate paramagnetism was observed down to 1.3 °K in gadolinium-yttrium alloys with even as much as 10 atomic percent gadolinium. On the other hand, solid solutions of gadolinium in thorium, another superconductor, were found to be ferromagnetic.

Thoburn et al. (41) have obtained magnetization data on gadolinium-lanthanum and gadolinium-yttrium alloys with rather large gadolinium concentrations. The gadolinium-lanthanum alloys with gadolinium concentrations from 46 percent to 83 percent were found to exhibit transitions to antiferromagnetism as the temperature was lowered. A transition to ferromagnetism occurred for each alloy at a temperature below the antiferromagnetic transition. The gadolinium-yttrium alloys with gadolinium concentrations from 25 percent to 60 percent were found to exhibit a transition to antiferromagnetism at a temperature that varied nearly linearly with gadolinium concentration. There was no evidence for a transition to ferromagnetism at lower temperatures for the 25 percent and 50 percent gadolinium-yttrium alloys.

From the experimental data on magnetic properties of dilute alloys that were available at the time this research was undertaken, it could be seen that none of those alloys studied exhibited properties of the type needed for adiabatic magnetization. Further, there did not seem to be any good way by which one could predict the magnetic properties of a new alloy system by using the results for a different alloy system. Thus a search was conducted to attempt to find an alloy that would be useful in adiabatic demagnetization.

Because of their high magnetic moment and the fact that the electrons contributing to their magnetism are, as stated by Van Vleck (42, p. 501),

"so deeply sequestered in the interior of the atom that they are well screened from interference by their neighbors", the rare earth metals were considered as good possibilities to use as solutes in dilute alloys for adiabatic demagnetization. In the work reported here the magnetic properties of alloys of certain rare earth metals with either yttrium or ytterbium were investigated. For reference, Table 1 lists the rare earth metals with some of their physical properties and atomic constants.

Two alloys of gadolinium with yttrium were studied. Yttrium was chosen as the host lattice because it has the same hexagonal close packed crystal structure and very nearly the same lattice parameters as gadolinium (44, p. 370). Gadolinium with a spin of  $7/2$  and  $g$  value of 2 was chosen because of its high effective magneton number and also because this metal is free of orbital magnetic effects. If the interaction between gadolinium ions is considered as a spin-spin

Table 1. Some physical properties and atomic constants of the rare earth metals.

Element	Atomic number	Atomic weight <sup>a</sup>	Crystal structure <sup>b</sup>	Number of conduction electrons	Number of 4f electrons	S	L	J	g	P <sub>eff</sub>	
										calc.	obs.
Y	39	88.9	hcp	3	0	-	-	-	-	-	-
La	57	138.92	hex	3	0	-	-	-	-	-	-
			fcc								
Ce	58	140.13	fcc	3	1	1/2	3	5/2	6/7	2.6	2.3 <sup>c</sup>
				4	0	-	-	-	-	-	-
Pr	59	140.92	hex	3	2	1	5	4	4/5	3.6	3.6 <sup>b</sup>
Nd	60	144.27	hex	3	3	3/2	6	9/2	8/11	3.6	3.7 <sup>b</sup>
Pm	61	(145)									
Sm	62	150.35	rhomb	3	5	5/2	5	5/2	2/7	1.6	2.1 <sup>c</sup>
Eu	63	152.0	bcc	2	7	7/2	0	7/2	2	7.9	8.3 <sup>c</sup>
Gd	64	157.26	hcp	3	7	7/2	0	7/2	2	7.9	7.9 <sup>b</sup>
Tb	65	158.93	hcp	3	8	3	3	6	3/2	9.7	9.0 <sup>b</sup>
Dy	66	162.51	hcp	3	9	5/2	5	15/2	4/3	10.6	10.2 <sup>b</sup>
Ho	67	164.94	hcp	3	10	2	6	8	5/4	10.6	10.9 <sup>b</sup>

<sup>a</sup>Hodgman et al. (43. pp. 353-4).

<sup>b</sup>Spedding et al. (44).

<sup>c</sup>Klemm and Bommer (45). The values for Ce and Sm are cited as a function of temperature. Room temperature values are quoted here.

Table 1. Some physical properties and atomic constants of the rare earth metals.

Element	Atomic number	Atomic weight <sup>a</sup>	Crystal structure <sup>b</sup>	Number of conduction electrons	Number of 4f electrons	$\chi_{eff}$					
						S	L	J	g	calc.	obs.
Y	39	88.9	hcp	3	0	-	-	-	-	-	-
La	57	138.92	hex	3	0	-	-	-	-	-	-
			fcc								
Ce	58	140.13	fcc	3	1	1/2	3	5/2	6/7	2.6	2.3 <sup>c</sup>
				4	0	-	-	-	-	-	-
Pr	59	140.92	hex	3	2	1	5	4	4/5	3.6	3.6 <sup>b</sup>
Nd	60	144.27	hex	3	3	3/2	6	9/2	8/11	3.6	3.7 <sup>b</sup>
Pm	61	(145)									
Sm	62	150.35	rhomb	3	5	5/2	5	5/2	2/7	1.6	2.1 <sup>c</sup>
Eu	63	152.0	bcc	2	7	7/2	0	7/2	2	7.9	8.3 <sup>c</sup>
Gd	64	157.26	hcp	3	7	7/2	0	7/2	2	7.9	7.9 <sup>b</sup>
Tb	65	158.93	hcp	3	8	3	3	6	3/2	9.7	9.0 <sup>b</sup>
Dy	66	162.51	hcp	3	9	5/2	5	15/2	4/3	10.6	10.2 <sup>b</sup>
Ho	67	164.94	hcp	3	10	2	6	8	5/4	10.6	10.9 <sup>b</sup>

<sup>a</sup>Hodgman et al. (43. pp. 353-4).

<sup>b</sup>Spedding et al. (44).

<sup>c</sup>Klemm and Bommer (45). The values for Ce and Sm are cited as a function of temperature. Room temperature values are quoted here.

Table 1. (Continued)

Element	Atomic number	Atomic weight <sup>a</sup>	Crystal structure <sup>b</sup>	Number of conduction electrons	Number of 4f electrons	S	L	J	g	P <sub>eff</sub>	
										calc.	obs.
Er	68	167.27	hcp	3	11	3/2	6	15/2	6/5	9.6	10.0 <sup>b</sup>
Tm	69	168.94	hcp	3	12	1	5	6	7/6	7.6	7.6 <sup>b</sup>
Yb	70	173.04	fcc	2	14	-	-	-	-	-	-
Lu	71	174.99	hcp	3	14	-	-	-	-	-	-

interaction after Néel (46), then the gadolinium-yttrium alloys would be a model by which interaction energies in other rare earth alloys could be determined.

Two alloys of holmium with yttrium and one alloy of dysprosium with yttrium were studied. Holmium and dysprosium have almost the same effective magneton numbers, each roughly half again as much as for gadolinium. Both have large orbital contributions to the magnetic moment. Holmium has a spin of 2 and dysprosium a spin of  $5/2$  so that magnetic interaction energies would be expected to be correspondingly less than in the case of gadolinium.

In order to learn something about the effect of the lattice on the dilute holmium system an alloy of holmium in ytterbium was studied. Ytterbium is divalent and has the face-centered cubic crystal structure (44, p. 370). To see whether the number of conduction electrons affected the magnetic interaction energy in these dilute alloys an alloy of europium in ytterbium was investigated. Europium has the body-centered cubic crystal structure, and ytterbium the face-centered crystal structure, and both are divalent. Divalent europium is in the same ground state as trivalent gadolinium so that one could expect to make a comparison between the properties of this alloy and a gadolinium-yttrium alloy of the same solute concentration.

The two holmium-yttrium alloys were studied in single crystal form in order to investigate anisotropy effects in the magnetic properties. The results of Hall et al. (47) on single crystals of yttrium show that there is a large anisotropy in the electrical resistivity. This suggested



that anisotropy effects might also be observed in the magnetization of dilute alloys with yttrium as the host lattice.

## BASIC CONCEPTS

## Thermodynamics of Adiabatic Demagnetization

In order to produce cooling it is necessary to have a working substance whose entropy depends both on the temperature and an externally variable parameter. The cooling is carried out in two steps: First, the entropy is reduced isothermally by adjusting the external parameter. Then the external parameter is varied isentropically in the opposite direction. In order for the system to retain its same degree of disorder, it is necessary for the temperature to lower.

Materials used in adiabatic demagnetization have the property that their entropy can be isothermally reduced by application of a magnetic field. In order for an effective proportion of the total entropy to be removed, however, it is necessary that the entropy due to lattice vibrations be small in comparison with the magnetic entropy of the system. This requires that the isothermal reduction of entropy by magnetization be done near 1.0 °K. The temperature of the system is then lowered by adiabatic demagnetization.

The entropy of the paramagnetic materials used in adiabatic demagnetization arises from the multiplicity of the ground state of the atomic systems. For a system of total angular momentum  $J$  there exist  $2J + 1$  states which are degenerate in the absence of a magnetic field, provided the temperature is considerably above the characteristic temperature of the system. This characteristic temperature is determined by the effects of the lattice (and conduction electrons in

the case of metals) on an atom in a solid, and is considerably less than 1 °K for paramagnetic salts used in adiabatic demagnetization. The magnetic entropy which can be removed at 1 °K is thus  $k \log(2J + 1)$  per atom. The orbital degeneracy associated with the quantum number  $J$  may be partially or wholly lifted by the effect of the crystalline electric field. If it is completely lifted, the magnetic entropy is then determined only by the spin  $S$  and is  $k \log(2S + 1)$  per atom.

The laws of thermodynamics applied to a substance in a magnetic field may be expressed as

$$TdS = dU + MdH \quad (1)$$

where  $T$  denotes absolute temperature,  $S$  the entropy per unit volume,  $U$  the internal energy per unit volume,  $M$  the magnetization per unit volume, and  $H$  the magnetic field strength. From this it can be shown that along an isentropic

$$C_H dT = - T \left( \frac{\partial M}{\partial T} \right)_H dH, \quad (2)$$

where  $C_H$  is the specific heat per unit volume at constant  $H$ . Thus the adiabatic demagnetization process will produce cooling if  $\left( \frac{\partial M}{\partial T} \right)_H$  is negative. This is the case with paramagnetic materials. It should be pointed out that materials which exhibit an antiferromagnetic transition have a positive  $\left( \frac{\partial M}{\partial T} \right)_H$  below the transition temperature so that warming would occur by adiabatic demagnetization, or cooling by adiabatic magnetization. The decrease in entropy during the isothermal magnetization at the initial temperature  $T_1$  is

$$S - S_0 = \int_0^H \left( \frac{\partial M}{\partial T} \right)_H dH, \quad (3)$$

where  $S$  is the entropy in the magnetic field and  $S_0$  is the zero field entropy. Since the cooling is produced through an isentropic change,  $S$  also represents the entropy of the system immediately after the demagnetization. Therefore

$$\int_0^H \left( \frac{\partial M}{\partial T} \right)_H dH = \int_{T_i}^{T_f} \frac{C_0}{T} dT, \quad (4)$$

where  $C_0$  is the zero field specific heat of the system and  $T_i, T_f$  are the initial and final temperatures, respectively.

#### Magnetic Fields in Material Media

The magnetic field  $H$  which is to be considered as the field acting on the magnetic ions of a paramagnetic material is not, in general, equal to the externally applied field. If the external magnetic field is uniform, the field within the material will be uniform if the material is in the shape of an ellipsoid. The relation between the internal field  $H_{int}$  and the externally applied field  $H_{ext}$  is then

$$H_{int} = H_{ext} - \mathcal{E} M. \quad (5)$$

$\mathcal{E}$  is the demagnetization factor and is determined by the shape of the material (48). For a prolate spheroid of an isotropic substance placed in a uniform external field

$$\mathcal{E} = 4\pi \frac{1-e^2}{e^2} \left[ \frac{1}{2e} \log \frac{1+e}{1-e} - 1 \right] , \quad (6)$$

where  $e$  is determined by the axial ratio and is given by

$$e = \sqrt{1 - \frac{a^2}{c^2}} , \quad (7)$$

$a$  being the major axis and  $c$  the axis of revolution.

According to the Lorentz model the local field  $H_{loc}$  acting on an individual ion is given by

$$H_{loc} = H_{ext} + \left( \frac{4}{3}\pi - \mathcal{E} \right) M . \quad (8)$$

On this basis the local susceptibility of the material, defined as the ratio of  $M$  to  $H_{loc}$  is

$$\chi_{loc} = \frac{M/H_{ext}}{1 + \left( \frac{4}{3}\pi - \mathcal{E} \right) M/H_{ext}} . \quad (9)$$

In the case of a spherical sample  $\mathcal{E} = 4\pi/3$ , and thus  $\chi_{loc} = \chi_{ext}$ , where  $\chi_{ext}$  is the ratio of the magnetization to the external field. The Lorentz approximation to the magnetic field assumes that all dipoles in the medium are equal and parallel. Although this is not true for a paramagnetic material the approximation holds quite well for  $\chi \ll 1$ .

#### Normal Paramagnetism

Materials which exhibit temperature dependent paramagnetism have a nonzero value of the total angular momentum  $J$  in the ground state. In

the absence of a magnetic field the ground state is  $2J + 1$  -fold degenerate. However with the application of a magnetic field  $H$  there will be a first-order Zeemann splitting of the levels with separation  $g\mu_B H$  where  $g$  is the Lande factor, and  $\mu_B$  is the Bohr magneton. A statistical treatment gives the following result for the magnetization  $M$  of  $N$  magnetic ions per unit volume:

$$M = NgJ\mu_B B_J(x) \quad . \quad (10)$$

$x$  is defined as  $gJ\mu_B H/kT$  and  $B_J(x)$  is the Brillouin function:

$$B_J(x) = \frac{2J+1}{2J} \coth\left[\frac{(2J+1)x}{2J}\right] - \frac{1}{2J} \coth \frac{x}{2J} \quad . \quad (11)$$

Values of this function and its first derivative have been tabulated by Schmid and Smart (49) for various  $J$  values. In the high temperature, low field limit for which  $x \ll 1$ ,

$$M = NJ(J+1)g^2\mu_B^2 H/3kT \quad , \quad (12)$$

which is Curie's law with the Curie constant given by

$$C = NJ(J+1)g^2\mu_B^2/3k \quad . \quad (13)$$

If the magnetic field that is used in Equation 12 is taken to be the local field given by Equation 8 then Curie's law for an ellipsoidal sample becomes

$$M = CH_{\text{ext}}/(T - \Delta) \quad , \quad (14)$$

where

$$\Delta = c \left( \frac{4\pi}{3} - \varepsilon \right) . \quad (15)$$

$\Delta$  is dependent on the shape of the sample and the Curie constant and ordinarily is considerably less than 1 °K.

It is convenient to speak in terms of an effective paramagnetic magneton number defined as

$$p_{\text{eff}} = [J(J+1)g^2]^{\frac{1}{2}} . \quad (16)$$

This gives the number of Bohr magnetons which contribute to the magnetization of a single atom. The saturation magnetization, obtained in the limit of large  $H/T$  is

$$M_{\text{sat}} = NgJ\mu_B . \quad (17)$$

A magneton number characteristic of the saturation magnetization per atom is defined as

$$n_{\text{eff}} = gJ . \quad (18)$$

### Ferromagnetism and Antiferromagnetism

Ferromagnetism is characterized by the presence in a material of a spontaneous magnetization in the absence of a magnetic field. The temperature above which this spontaneous magnetization disappears is called the Curie temperature. Above the Curie temperature ferromagnetic materials exhibit paramagnetic behavior and follow a Curie-Weiss law:

$$M = CH/(T - \Theta) \quad . \quad (19)$$

In this expression  $\Theta$  is called the paramagnetic Curie temperature and is usually somewhat larger than the actual transition temperature. On the basis of the Weiss molecular field theory the saturation magnetic moment is obtained from Equation 10 in the limit of large  $H/T$ . The saturation magnetization is given by Equation 15 and the effective magneton number by Equation 16.

Antiferromagnetism in a substance is characterized by an antiparallel orientation of neighboring spins. The most characteristic property of a polycrystalline antiferromagnetic substance is that its susceptibility shows a maximum as a function of temperature. The temperature at which the antiparallel alignment begins to occur is called the Néel temperature, and above this temperature the magnetic spins are "free" and exhibit paramagnetism described by the Curie-Weiss law of Equation 16 with  $\Theta$  replaced by  $-\Theta$ . In absolute magnitude this value of  $\Theta$  is very nearly equal to the Néel temperature.



## MATERIALS TESTED

## Preparation

The pure metals used in fabricating the alloys were prepared in this laboratory. The rare earth metals were obtained in distilled form by reduction from the fluoride using techniques developed by Spedding and Daane (50). Yttrium metal was prepared by a method described by Spedding et al. (51). The yttrium metal was taken directly from a sponge obtained in the final separation process.

Alloys of yttrium with small amounts of rare earth metal were prepared by arc melting together in a helium atmosphere the proper amounts of each constituent in the following manner: Two separate buttons were formed, each containing half the proper amounts of the two metals to be alloyed. These buttons were separately flipped over and remelted six times, then melted together into a larger button which, in turn, was flipped over and remelted six times. The resulting alloy was formed into approximately the desired shape by building up a long narrow button in layers. Alloys of ytterbium with rare earth metals were prepared by casting together the proper amounts of each metal in a tantalum crucible. The probability of obtaining homogeneous alloys with both of these methods is very good.

The alloys were fabricated into the desired form by machining on a lathe. The two gadolinium-yttrium samples were cut into the shape of a prolate spheroid of diameter  $5/8$  inch and length  $1-1/2$  inch. The remainder of the samples were cut into cylinders  $1-1/2$  inch long and  $5/8$

inch diameter.

### Single Crystals

Single crystals were obtained for two alloys of holmium-yttrium. The method employed in producing these single crystals was a grain growth technique which has been described by Hall et al. (47). An arc-melted slug of the alloy was carefully polished and subsequently annealed in a vacuum at about 1250 °C for 24 hours. The resulting specimen consisted usually of several grains, some of which were as large as 3mm by 3mm by 9mm. Crystal orientation was determined by standard back reflection x-ray technique as described by Greninger (52). The surfaces of the grains immediately after the anneal were of a quality good enough to allow excellent x-ray pictures to be taken without etching.

The single crystals were cut from the annealed slug with a jeweler's saw and ground and polished into shape on emery paper. The single crystal of Ho-Y 0.6-99.4 was shaped into an approximate rectangular parallelepiped of dimensions 3mm by 5mm by 6mm and mass 0.408 gram. The single crystal of Ho-Y 1.0-99.0 was shaped into a rectangular parallelepiped of dimensions 3.1 mm by 3.1 mm by 9.1 mm and mass 0.400 gram. The length of this latter crystal was in the direction of the c-axis. (The symbols used above to designate the samples are explained in the next section.)

### Purity

Each of the metals used to prepare the various alloys was examined spectrographically for impurities, except for the gadolinium on which no

analysis is available. In addition the single crystals of holmium-yttrium alloys were tested spectrographically for metal ion impurity and by vacuum fusion for dissolved oxygen.

Two gadolinium-yttrium alloys were studied in this investigation. These will be designated Gd-Y 0.3-99.7 and Gd-Y 1.0-99.0, and they contained 0.3 and 1.0 atomic percent gadolinium, respectively. The analysis for the yttrium used in preparing these alloys is given in Table 2.

Table 2. Analysis of yttrium used in preparation of the gadolinium-yttrium alloys.

Element	Content in yttrium (%)
C	.012
N	.016
F	.118
O	.13
Ta	<.01
Ti	<.005
Ni	~.02
Mg	<.0015
Fe	~.02

From the analysis it can be seen that the oxygen impurity is significantly high. The effect of this on the magnetic properties of the alloy will be discussed in a later section.

Two holmium-yttrium alloys with holmium content 0.6 and 1.0 atomic

percent were studied. These will be designated as Ho-Y 0.6-99.4 and Ho-Y 1.0-99.0, respectively. The analysis for the metals used to prepare these alloys is shown in Table 3.

Table 3. Analysis of holmium and yttrium used in preparation of holmium-yttrium alloys.

Element	Content in holmium (%)	Content in yttrium (%)
C	.0075	.0089
N	.0094	.0020
F		.0071
O		.020
Ca	.05	< .001
Ta	< .1	~ .01
Ti		very low
Zr		very low
Fe	.01	~ .02
Ni		~ .02
Si	< .02	
Tm	< .01	
Er	< .01	
Dy	.04	

One dysprosium-yttrium alloy was studied. It contained 1.0 atomic percent dysprosium and is to be designated as Dy-Y 1.0-99.0. The analysis for the metals used in preparing this alloy is shown in Table 4.

One alloy of holmium in ytterbium and one of europium in ytterbium were investigated. The concentrations were 1.25 atomic percent holmium and 0.4 atomic percent europium for which the respective designations are

Table 4. Analysis of dysprosium and yttrium used in preparation of the dysprosium-yttrium alloy.

Element	Content in dysprosium (%)	Content in yttrium (%)
C	.01	.0063
N	.0015	.0006
F		.0072
O	.013	.0425
H	.015	
Ca	.05	.0001
Ta	.1	
Si	.03	
Fe	.01	~ .02
Er	.02	
Ho	.02	
Tb	.1	
Yb	.005	
Mg		.00014
Ni		~ .02

Ho-Yb 1.25-98.75 and Eu-Yb 0.4-99.6. The ytterbium for both alloys was from the same source so the analysis for the metals for both alloys is given in Table 5.

Single crystals were studied for the two holmium-yttrium alloys already mentioned. Small pieces from each of these crystals were analyzed for impurity. The results are indicated in Table 6.

The observed holmium concentrations of 1.13 and 2.05 percent by weight become 0.61 percent and 1.11 percent, respectively, on an atomic basis. To within the 10 percent accuracy of the spectrographic analysis,

Table 5. Analysis of holmium, europium, and ytterbium used in preparation of holmium-ytterbium and europium-ytterbium alloys.

Element	Content in holmium (%)	Content in europium (%)	Content in ytterbium (%)
C	.0065		.0090
N	.0019		.0052
F	.050		.0030
Ca	<.05	trace	.05
Fe	<.01		<.05
Ta	<.1	~.1	<.1
Si	.02		<.01
Y	<.01		
Dy	<.04		
Er	<.01		
Tm	<.01		
Yb		faint trace	
La			trace
Sm		faint trace	
Mg			<.01

Table 6. Analysis of single crystals of Ho-Y 0.6-99.4 and Ho-Y 1.0-99.0.

Element	Content in Ho-Y 0.6-99.4 (%)	Content in Ho-Y 1.0-99.0 (%)
O	.025	.028
Al	trace	faint trace
Cu	trace	very weak
Fe	very weak	very weak
Ho	$1.13 \pm .11$	$2.05 \pm .20$
Mg	faint trace	not detected
Ni	trace	very weak
Si	faint trace	faint trace
Er	$\leq .005$	$\leq .005$
Dy	$\leq .005$	$\leq .005$
Tb	$\leq .05$	$\leq .05$
Gd	$.08 \pm .04$	$.08 \pm .04$
Sm	$\leq .05$	$\leq .05$
Ca		trace

these values are in good agreement with the percentages 0.60 and 1.00, respectively, determined from the weights of the constituents used in the alloying.

## EXPERIMENTAL PROCEDURE

### Magnetic Susceptibility Measurements

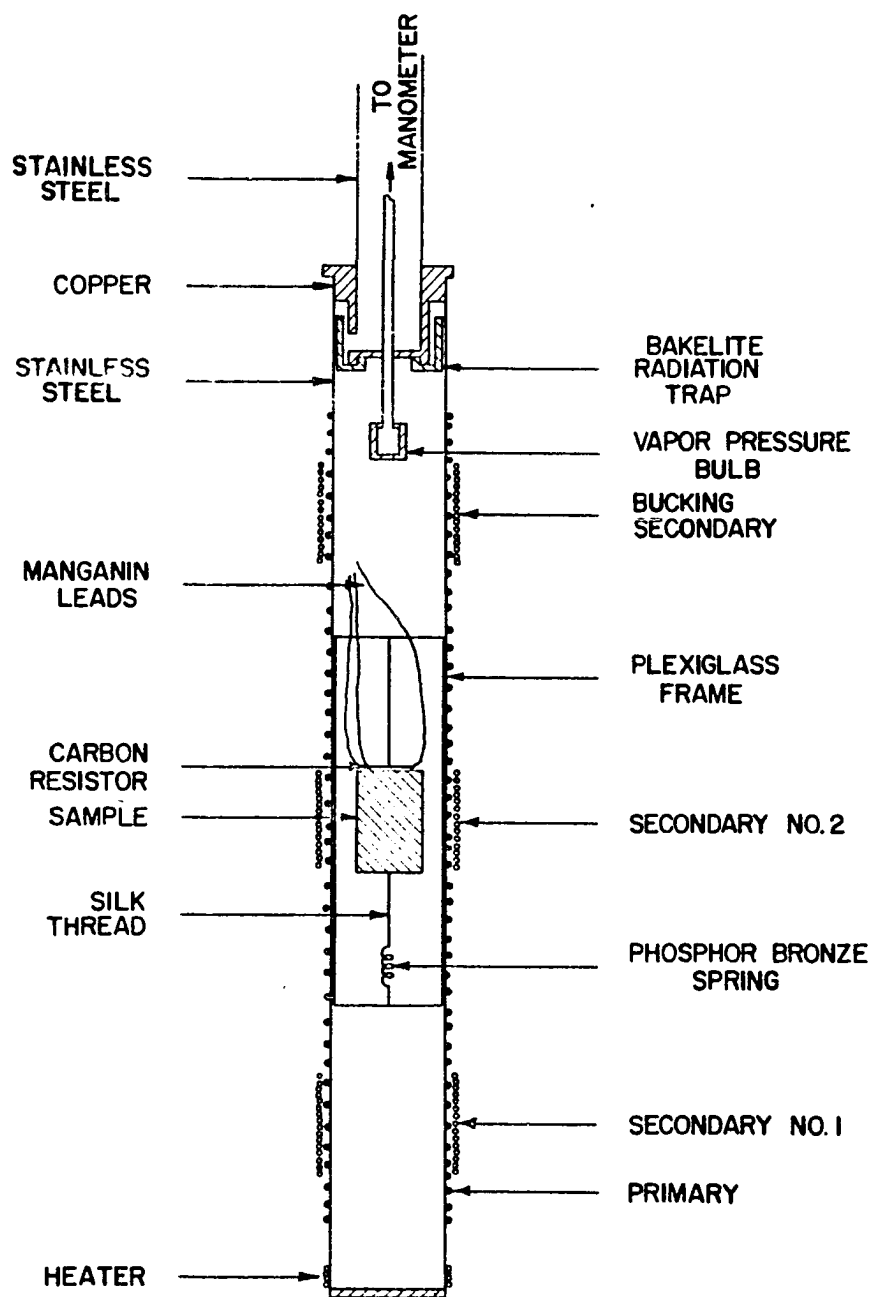
The magnetic susceptibility was measured in the liquid helium temperature range for all samples except the single crystals of holmium-yttrium and the polycrystalline sample of europium-ytterbium. The method used was insensitive to samples as small as the single crystals of holmium-yttrium. The europium-ytterbium sample exhibited large remanence characteristic of a ferromagnetic material so that susceptibility measurements could not be obtained for this sample. As described later, measurements on some samples were made at temperatures below 1 °K.

A metal helium cryostat of the type described by Henry and Dolecek (53) was used in this work. A modification was made to the tail assembly of the cryostat in order to reduce the effects of eddy currents on the susceptibility measurements. The inner and outer sections of the tail assembly were made of stainless steel. The copper radiation shield in the tail had a narrow slit along its full length in order to present an open electrical circuit to eddy currents attempting to flow circularly around the copper tube. In order to keep room temperature radiation from passing through this slit and striking the liquid helium dewar, the radiation shield was wrapped with a layer of aluminum foil.

The detail of the sample tube used for the susceptibility measurements is shown in Figure 1. The sample was suspended in the sample tube by fine silk threads, as illustrated, for some of the runs. This was done in order that data on adiabatic demagnetization could be



Figure 1. Sample tube used for susceptibility measurement.



obtained during the same liquid helium run. Other susceptibility measurements for all samples were made with the sample centered in the sample tube with bakelite spacers. In each case the sample was brought to the temperature of the liquid helium bath by the introduction of helium exchange gas into the sample tube at a pressure of 50-100 microns. The radiation shield at the top of the sample tube prevented room temperature radiation from above from entering the sample chamber.

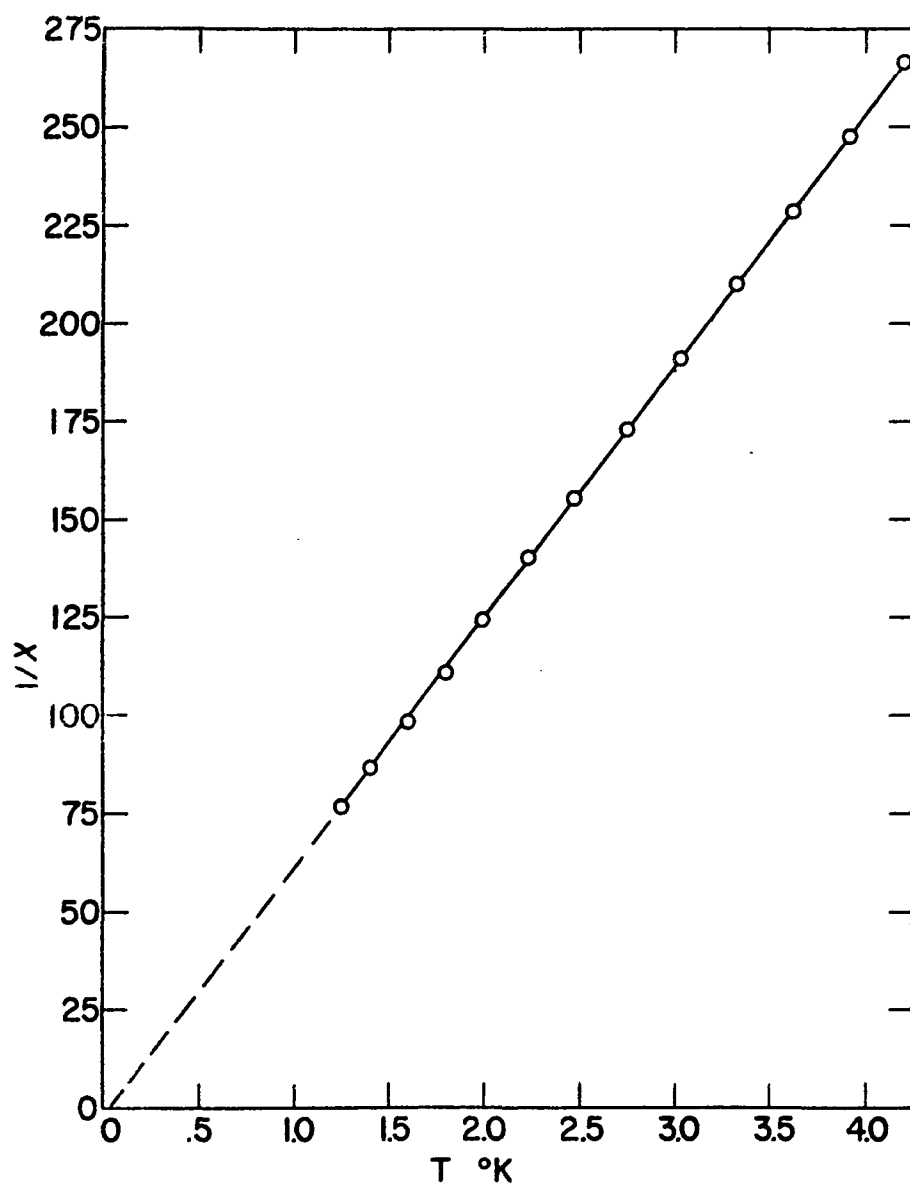
The temperature of the sample was taken as the temperature of the liquid helium bath at the same height in the helium dewar as the sample. The temperature of the liquid helium bath was determined by measuring the pressure over the bath with a mercury manometer for pressures greater than about 5 cm Hg, and with a butyl phthalate manometer for pressures less than this. Several separate calibrations showed the relative densities of the mercury and the butyl phthalate to be 12.98 and 1, respectively. At temperatures above 2.17 °K a suitable correction was made for the hydrostatic head between the top of the bath and the median plane of the sample. At temperatures below 2.17 °K, which is the  $\lambda$  - point of liquid  $\text{He}^4$ , the bath is very nearly a super heat conductor so that no such correction should be applied (54). The hydrostatic head correction above 2.17 °K was obtained as follows: A small amount of helium gas was condensed in a bulb located 4 inches above the median plane of secondary number 2 and 8 inches above the median plane of secondary number 1 (refer to Figure 1). A 1/16 inch diameter stainless steel tube connected this bulb with a line leading to a manometer system. The difference between the pressure over the

bath and the vapor pressure in the bulb was observed with a butyl phthalate manometer. The hydrostatic head correction was taken as the sum of this pressure difference and the hydrostatic head of liquid helium, corresponding to a depth of 4 inches for the central position and 8 inches for the lower position in the sample chamber. The temperature was then obtained from the "1958 He<sup>4</sup> Scale of Temperatures" (54).

As a check on temperature measurement and also for calibration purposes, several runs were made with a sample of a paramagnetic salt. A plot of inverse susceptibility versus temperature obtained for an ellipsoidal compressed pill of iron ammonium alum is shown in Figure 2. The experimental points fit a straight line very well, as expected from Curie's law. The intercept of 0.04 °K on the temperature axis agrees well with the value of  $\Delta = 0.036$  °K computed from Equation 15. It can be concluded that the method of temperature measurement is good.

Susceptibility was measured with a ballistic Hartshorn bridge which was patterned after one described by deKlerk and Hudson (55). A ballistic method of measurement was chosen because it was felt that an A. C. method would induce undesirable eddy currents in the metal samples making the interpretation of the susceptibility difficult. The galvanometer chosen for this arrangement had a sensitivity of 0.05 microvolt per mm at 1 meter, a period of 5 seconds, and an external critical damping resistance of 8 ohms. The primary and secondary detection coils were wound directly on a 7/8 inch diameter stainless steel sample tube of 0.011 inch wall thickness. The primary consisted of a single layer of 1498 close-wound turns of 34 gauge triple formvar

Figure 2. Inverse susceptibility versus temperature  
for an ellipsoidal compressed pill of  
iron ammonium alum.



copper wire. Each of the secondary coils was close-wound about the primary in four equal layers with 1304 turns of 39 gauge triple formvar copper wire.

The relative spacing of the secondary units is illustrated in Figure 1, which is a scale drawing of the sample tube. The secondary coil at the top of the sample tube serves to "buck out" a signal from either of the lower two coils so that no galvanometer deflection will be obtained if the sample tube is empty. The leads from secondaries number 1 and number 2 were led to a switch so that either of these could be connected into the bridge circuit. By this arrangement the susceptibility of two different samples could be measured during the same liquid helium run.

In taking measurements to determine susceptibility the following procedure was used: A steady current of 100 ma was maintained in the primary circuit. This current was reversed quickly and the resultant deflection of the galvanometer observed. External mutual inductance coils could be switched into the bridge circuit in opposition to the detection coils in order to keep the galvanometer deflection on scale. The switching circuit was arranged so that the detection sensitivity was unaffected by this. At any particular temperature, then, the effective galvanometer deflection was observed for reversal of a known current in the primary.

Calibration data were obtained for two differently shaped samples of a paramagnetic salt whose Curie constant was well known. The salt used for these measurements was iron ammonium alum of "Baker Analyzed"<sup>a</sup>

---

<sup>a</sup>Manufactured by J. T. Baker Chemical Co., Phillipsburg, N. J.

grade. Crystals of the salt were ground into a fine powder and compressed into a cylindrical pill of  $5/8$  inch diameter with a pressure of about 10,000 pounds per square inch. One sample for the calibration data was used in this cylindrical form with dimensions  $5/8$  inch diameter by  $1-1/2$  inch long. The second sample was cut on the lathe into an ellipsoid of  $5/8$  inch diameter by  $1-1/2$  inch long. Since this salt decomposes quite rapidly at room temperature, it was necessary to keep the samples well below the ice point while working with them. The ellipsoid sample was kept cold during the cutting process by allowing a spray of liquid nitrogen to fall on it all the time. The samples were stored by wrapping in aluminum foil and placing in a container of liquid nitrogen. The filling factor for each sample was determined by volume and mass determinations with the sample in cylindrical shape. The density as so determined was compared with the accepted value for crystalline density of  $1.71 \text{ g per cm}^3$  (43, p. 473). The filling factor as so determined was 0.97 for each sample.

The susceptibility of a metal alloy sample was determined by obtaining data of galvanometer deflection versus temperature and using the paramagnetic salt calibration data for the shape of that particular sample. The temperature range covered was  $1.2 \text{ }^\circ\text{K}$  to  $4.2 \text{ }^\circ\text{K}$ ; however, lower temperatures were obtained for two of the samples by magnetic cooling. The Gd-Y 0.3-99.7 alloy was cooled below the helium bath temperature by adiabatic demagnetization. The temperature was obtained from a calibrated carbon resistor mounted directly on the sample with



G. E. adhesive number 7031<sup>a</sup>. For this alloy, data of susceptibility versus temperature were obtained down to 0.84 °K. The carbon resistor used in this work was a Speer<sup>b</sup> nominal 470 ohm 1/2 watt resistor with the outer plastic casing removed in order to reduce its heat capacity. The resistance was measured with a three wire Wheatstone bridge connected in a manner that eliminated effects of lead-wire resistance.

The Ho-Y 1.0-99.0 alloy was cooled below the helium bath temperature with a compressed pill of iron ammonium alum by adiabatic demagnetization of the iron alum salt pill. A copper fin assembly was silver-soldered to a copper rod. The iron alum was ground into a fine powder and pressed into the fin assembly with a pressure of about 10,000 pounds per square inch. A small amount of toluene was added to the salt powder before it was compressed in order that the powder would flow properly when pressure was applied. The end of the copper rod of this assembly was then screwed tightly into the end of the metal sample and placed in a sample suspension as illustrated in Figure 3. A carbon resistor of the type described above was mounted on the copper rod to serve as a temperature monitor.

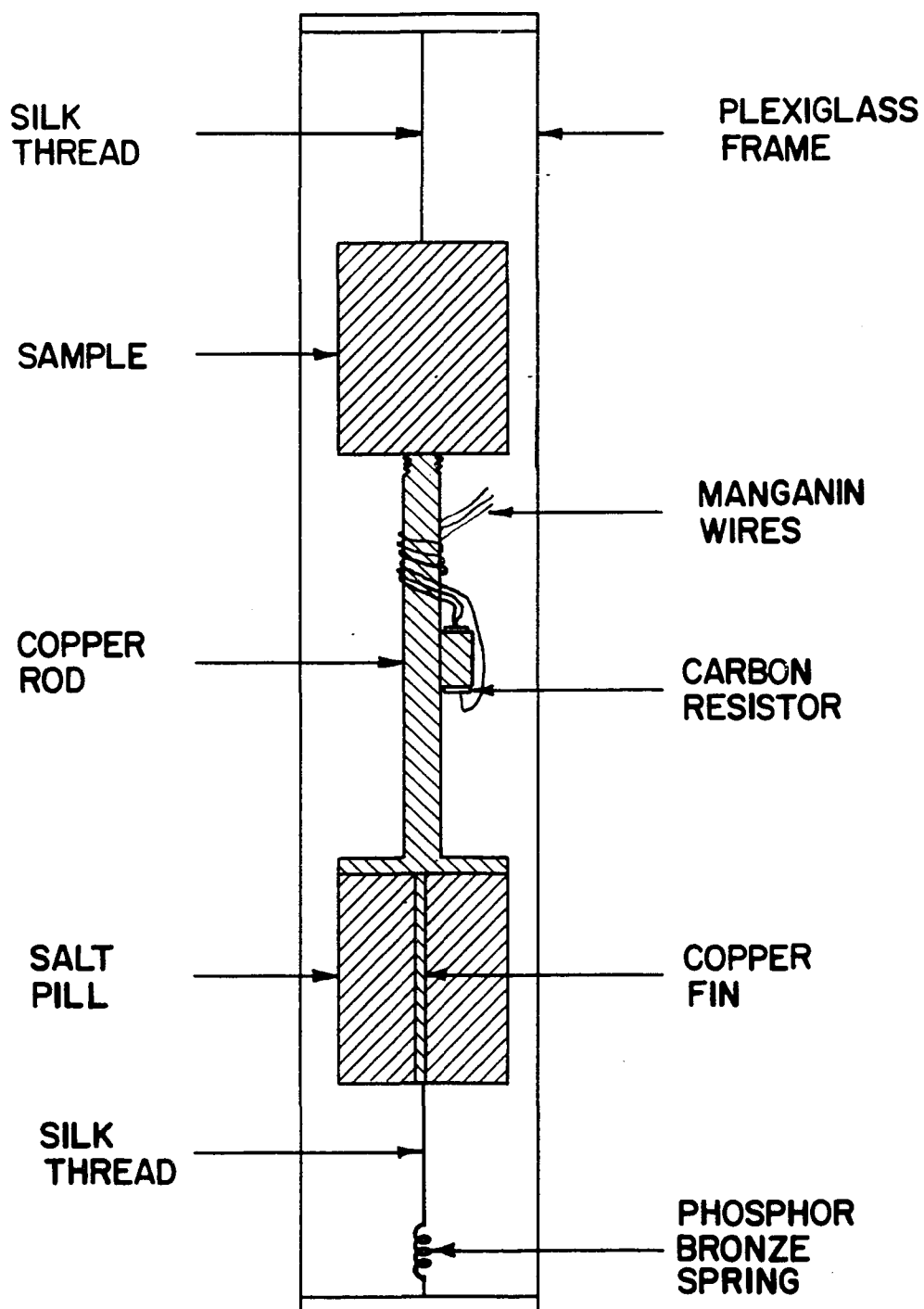
The temperature of the sample was obtained from the susceptibility of the iron ammonium alum by extrapolating the straight line plot of inverse susceptibility versus temperature into the region of temperature below 1 °K. The so-called Curie temperatures thus obtained were

---

<sup>a</sup>Manufactured by General Electric Co., Chemical Division, Pittsfield, Massachusetts.

<sup>b</sup>Manufactured by Speer Resistor Co., Bradford, Pennsylvania.

Figure 3. Sample assembly for cooling a sample by the adiabatic demagnetization of a paramagnetic salt.



converted to temperatures on the absolute scale with the correlation data of Cooke et al. (56) for iron ammonium alum.

### Magnetization Measurements

The magnetization of the single crystals of the holmium-yttrium alloys was measured at temperatures in the liquid helium region. The measurements were made using a 3 kw Weiss-type magnet that produced a uniform field gradient in the vertical direction for fields from 0 to 11 koe. The magnet and associated measuring equipment were patterned after the design of Elliott (57) as modified by Thoburn (58). Temperatures in the liquid helium region were obtained by pumping on a bath of liquid helium in a metal cryostat. The cryostat was similar to that used for the susceptibility measurements except that all parts in the tail assembly were made of copper.

A line drawing of the experimental arrangement is shown in Figure 4 and a more detailed drawing of the sample chamber in Figure 5. Helium exchange gas at a pressure of about 1 mm Hg was introduced into the bell jar and sample chamber in order that the sample would make good thermal contact with the liquid helium bath. (Helium exchange gas at a pressure of about 200 microns was introduced into the space between the sample chamber and the liquid bath. The apparatus was designed with this space so that temperatures above the bath temperature could be obtained by evacuating this chamber and dissipating power in the heater coil. No measurements at temperatures above the bath were made for the present research, however.) In order to reduce the heat leak to the

Figure 4. Experimental arrangement for magnetization measurements.

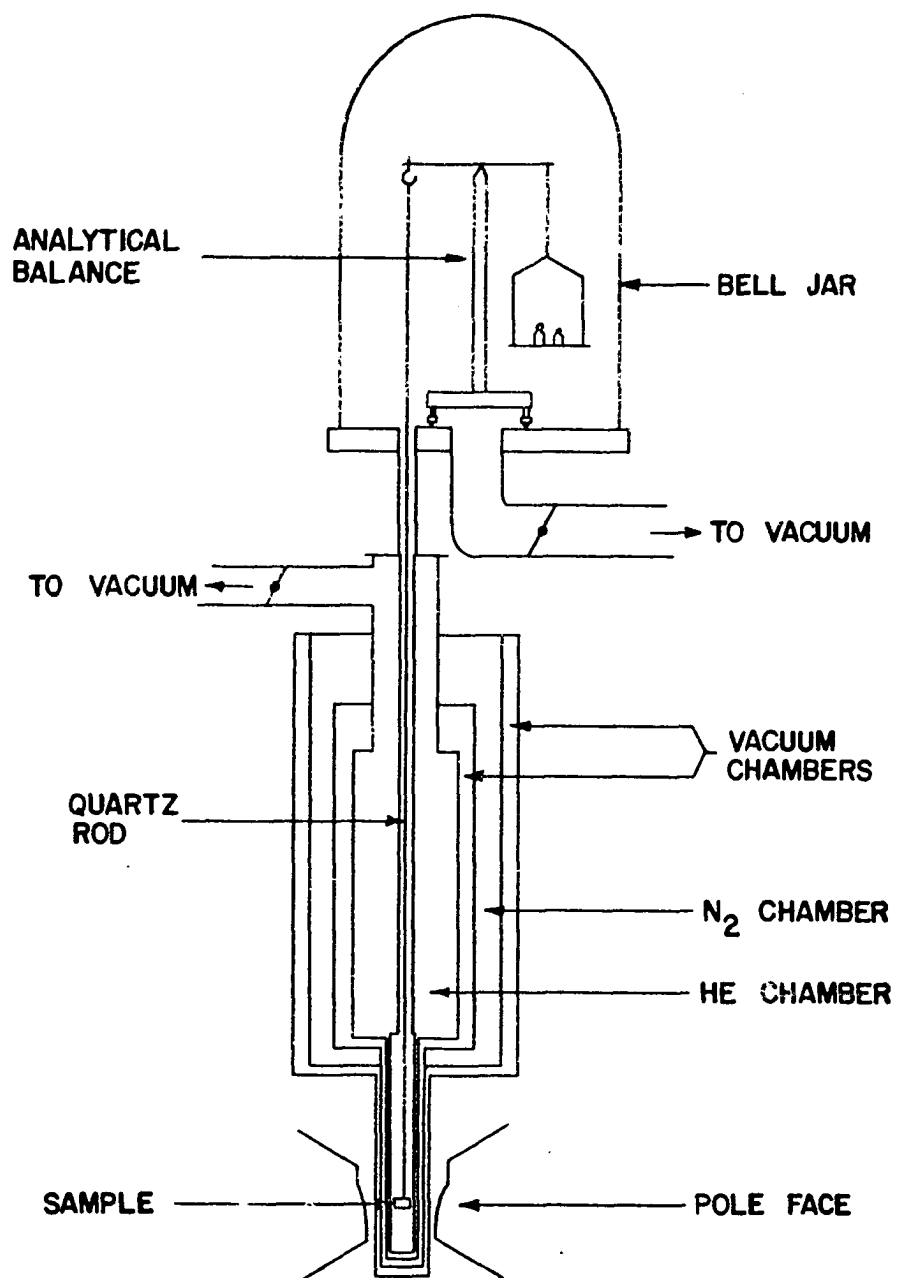
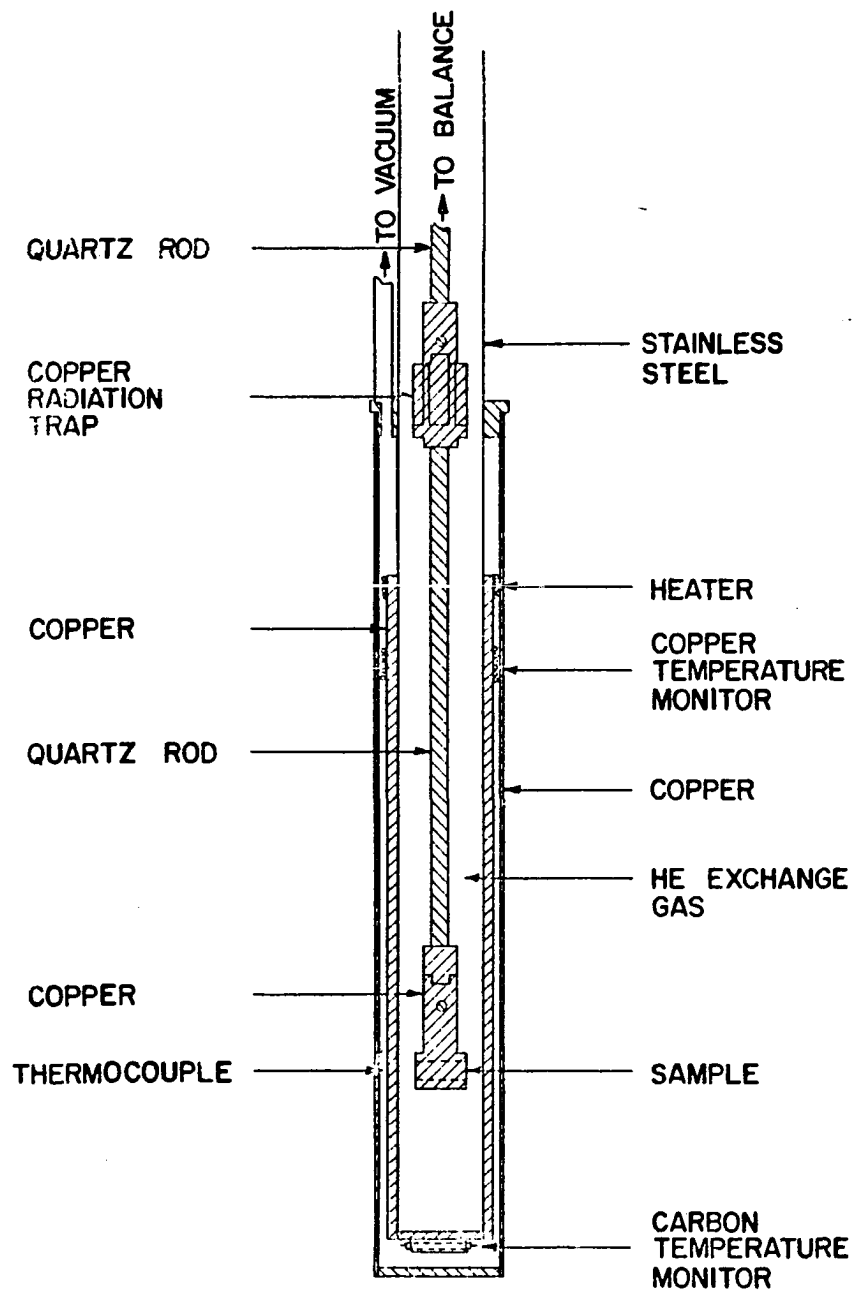


Figure 5. Detail of sample chamber used  
in magnetization measurements.





sample, the inside of the sample tube was blackened with Aquadag<sup>a</sup> so that it would absorb any radiation striking it. Room temperature radiation from above could then reach the bottom of the sample tube only by travelling in a straight line. In order to intercept part of this straight-line radiation, a copper radiation shield was introduced into the sample rod about 8 inches above the sample. The diameter of the shield was 1 cm which allowed it to cast a shadow on the entire sample and sample holder. Furthermore, the copper shield served as an effective heat station to conduct away to the exchange gas any small amount of heat that could be flowing down the quartz rod.

With the above-mentioned precautions, the sample was in very good thermal contact with the liquid helium bath. The temperature was determined by measurement of the pressure over the bath with a manometer system as described above, and reference to the "1958 He<sup>4</sup> Scale of Temperatures" (54).

#### Adiabatic Demagnetization Measurements

The metal alloys which exhibited paramagnetic behavior down to the lowest temperatures measured were examined by adiabatic demagnetization in order to see whether they would be useful in magnetic cooling. The sample tube and cryostat were the same as used in the susceptibility measurements. The sample tube with a sample mounted for demagnetization work is shown in Figure 1. The magnet was the same one used for the

---

<sup>a</sup>Manufactured by Acheson Colloids Corporation, Port Huron, Michigan.

magnetization measurements with the exception that plane pole pieces were used in order to produce a uniform magnetic field over the volume of the sample. The equipment for adiabatic demagnetization was mounted on one side of the room, that for magnetization measurements on the other. The magnet was mounted on wheels and could be rolled on rigid tracks from one setup to the other.

The sample was suspended at the center of a very thin-walled plexi-glass frame by two fine silk threads. The lower thread was attached to a phosphor bronze spring in order to reduce vibrations of the sample. A Speer carbon resistor of nominal value 470 ohms was mounted directly on the sample with G. E. adhesive as shown in Figure 1. Three 40 gauge manganin wires made electrical connection between the resistor and one arm of a Wheatstone bridge circuit. All the plastic covering was ground off the resistor to reduce its heat capacity, and one side was then ground flat so that it would make good physical contact with the sample. In order to attach the resistor to the Gd-Y 0.3-99.0 sample, it was necessary to fit one side of it to the curved surface of the ellipsoidal sample.

The purpose of the carbon resistor was to serve as a thermometer. Nicol and Soller (59) have shown that this type of resistor may be expected to have the following temperature-resistance relation between 4.2 and 0.3 °K:

$$A \log R = T (\log R - B)^2 \quad . \quad (20)$$

In this expression  $R$  is the resistance and  $T$  the temperature;  $A$  and

B are constants. The resistor used in this work was calibrated in the liquid helium region during each run, and temperatures below the bath temperature were determined from an extrapolation of this calibration curve. The R versus T relation of Equation 20 was checked for temperatures below the bath during two separate runs by cooling the resistor with a paramagnetic salt in an arrangement similar to that shown in Figure 3. The resistor was assumed to be in thermal equilibrium with the paramagnetic salt whose temperature was obtained from its susceptibility in a manner described above. The agreement was better than 5 percent down to 0.7 °K and better than 10 percent from 0.7 to 0.3 °K. Below 0.3 °K the value of temperature calculated from Equation 20 was found to deviate upwards very strongly from the temperature measured by the paramagnetic salt.

During the course of a demagnetization experiment the following procedure was used: Helium exchange gas at a pressure of about 10 microns was introduced into the sample chamber. The sample was magnetized at about 1.25 °K by application of a steady field of about 11 koe. As soon as the heat of magnetization had been carried away by the exchange gas, the sample chamber was pumped out to a vacuum of  $10^{-6}$  mm Hg or better. This pumping usually took about one hour. The magnetic field was then reduced to zero over a time interval of about 60 seconds. The demagnetization was done slowly in order that a minimum of eddy current heating would be induced in the sample. The magnet was then rolled away in order to remove the large amount of iron from the measuring coils of the ballistic bridge. The susceptibility

and resistance were measured every half minute after the demagnetization, as described above.

The demagnetization setup for the single crystals of Ho-Y 0.6-99.4 and Ho-Y 1.0-99.0 was similar to the arrangement described above. However an Allen-Bradley<sup>a</sup> deciwatt nominal 10 ohm resistor was mounted on the sample rather than the resistor used previously. This resistor was used in these measurements because of its extremely small size and mass (7 milligrams after being ground down) and consequent small heat capacity. In the liquid helium range of temperatures the resistance-temperature relation was found to obey Equation 20. Extrapolation to temperatures below 1 °K was used to obtain the temperature of the resistor and sample. The work of Clement et al. (60) on 10 ohm Allen Bradley resistors indicates that this relation holds true in the temperature interval 0.15 to 4.2 °K.

---

<sup>a</sup>Manufactured by Allen Bradley Company, Milwaukee, Wisconsin.

## RESULTS

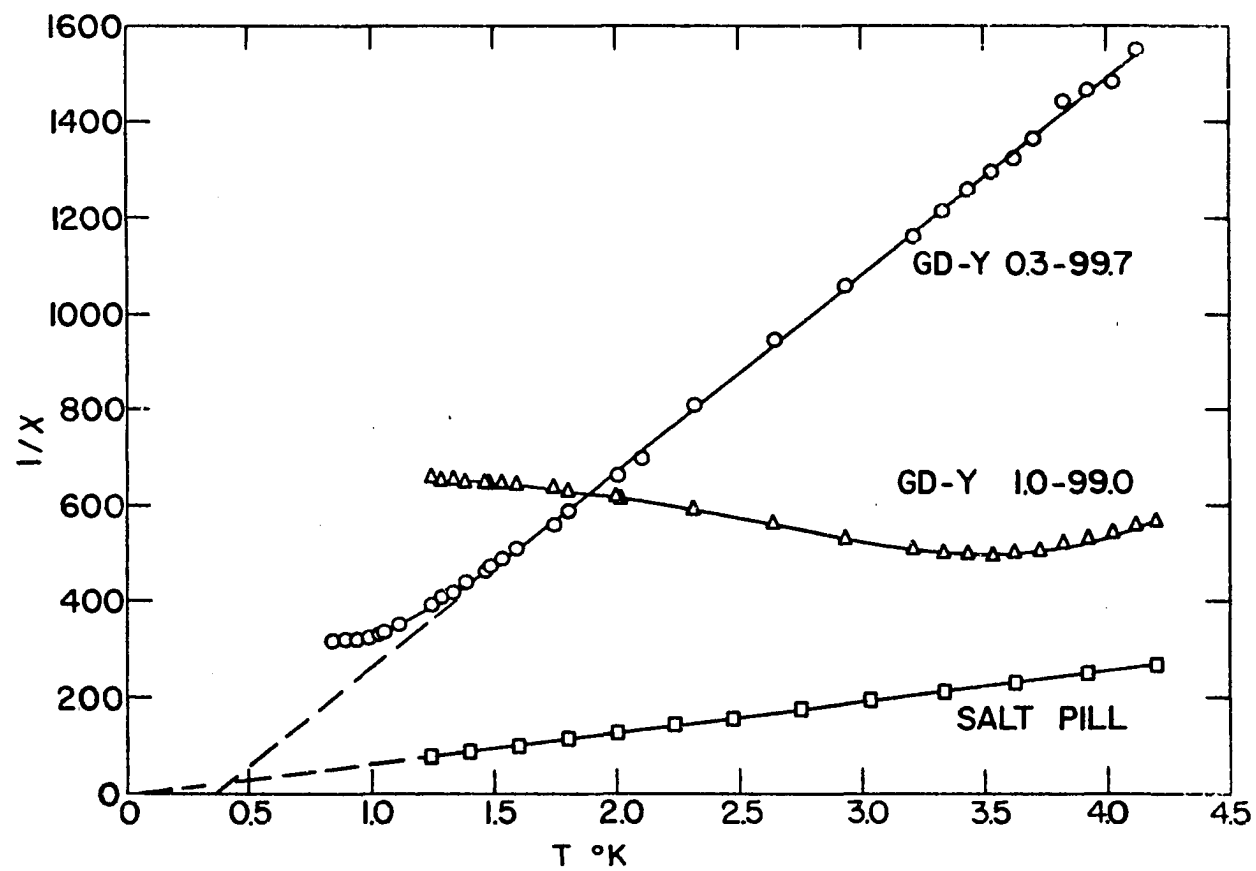
## Susceptibility Measurements

The magnetic susceptibility of two gadolinium-yttrium alloys was measured. The samples were in the form of ellipsoids  $5/8$  inch diameter by  $1-1/2$  inch long, and had gadolinium concentrations of 0.3 and 1.0 atomic percent. The data are plotted on the graph of Figure 6 in which the inverse susceptibility in cgs units is plotted as ordinate against temperature in degrees Kelvin as abscissa. Also presented for comparison are the data obtained for a compressed pill of iron ammonium alum. This pill had the same shape and dimensions as the alloy samples and was 0.97 of the crystalline density.

The Gd-Y 0.3-99.7 alloy exhibits paramagnetism down to the lowest measured temperature of  $0.84^{\circ}\text{K}$ , however the experimental points begin to deviate from a straight line at about  $1.5^{\circ}\text{K}$ . There is a strong indication that a maximum in susceptibility may occur not too far below  $0.84^{\circ}\text{K}$ . From the slope of the straight line portion of the plot, a Curie constant  $C = 0.0023$  was obtained. The intercept of the extrapolated straight line with the temperature axis is  $0.35^{\circ}\text{K}$ . The scatter in the experimental points near  $4.0^{\circ}\text{K}$  is very likely due to the insensitivity of the detection system to such a weakly magnetic material. The actual galvanometer deflection at  $4.2^{\circ}\text{K}$  was 8 mm with an uncertainty in measurement of 0.2 mm.

The Gd-Y 1.0-99.0 alloy shows a minimum in the plot of inverse susceptibility versus temperature, the minimum occurring at  $3.4^{\circ}\text{K}$ .

Figure 6. Inverse susceptibility versus temperature for the alloys Gd-Y 0.3-99.7 and Gd-Y 1.0-99.0. Data for a salt pill of iron ammonium alum are shown for comparison. See text.



This means that a maximum occurs in the susceptibility at this temperature; such behavior is characteristic of a transition to the antiferromagnetic state below this temperature. There are insufficient experimental data above the transition temperature for a determination of the Curie constant and paramagnetic Curie temperature.

The magnetic susceptibility of one dysprosium-yttrium alloy was measured. The sample contained 1.0 atomic percent dysprosium and was in the form of a cylinder  $5/8$  inch diameter by  $1-1/2$  inch long. The experimental data are presented in the graph of Figure 7 with inverse susceptibility plotted versus temperature. Similar data for a compressed pill of iron ammonium alum are shown for comparison. This pill was 0.97 of the crystalline density and was of the same shape and dimensions as the alloy specimen. The alloy exhibits simple paramagnetism down to about  $1.5^\circ\text{K}$ . However below this temperature there is a minimum in inverse susceptibility and thus a maximum in susceptibility; the susceptibility maximum occurs at  $1.34^\circ\text{K}$ . The Curie constant obtained from the straight line portion of the curve through the data points is  $C = 0.0076$ . The intercept of the extrapolated straight line with the temperature axis is  $-0.28^\circ\text{K}$ .

The magnetic susceptibility of two holmium-yttrium alloys was measured. One sample contained 0.6 atomic percent holmium, the other 1.0 percent; both were cylinders  $5/8$  inch diameter and  $1-1/2$  inch long. The experimental points are plotted on the graph of Figure 8 with inverse susceptibility versus temperature. The data for the salt pill are the same as presented in the graph of Figure 7 and are shown for comparison. Both alloys exhibit paramagnetic behavior down to the



Figure 7. Inverse susceptibility versus temperature for the alloy Dy-Y 1.0-99.0. Data for a salt pill of iron ammonium alum are shown for comparison. See text.

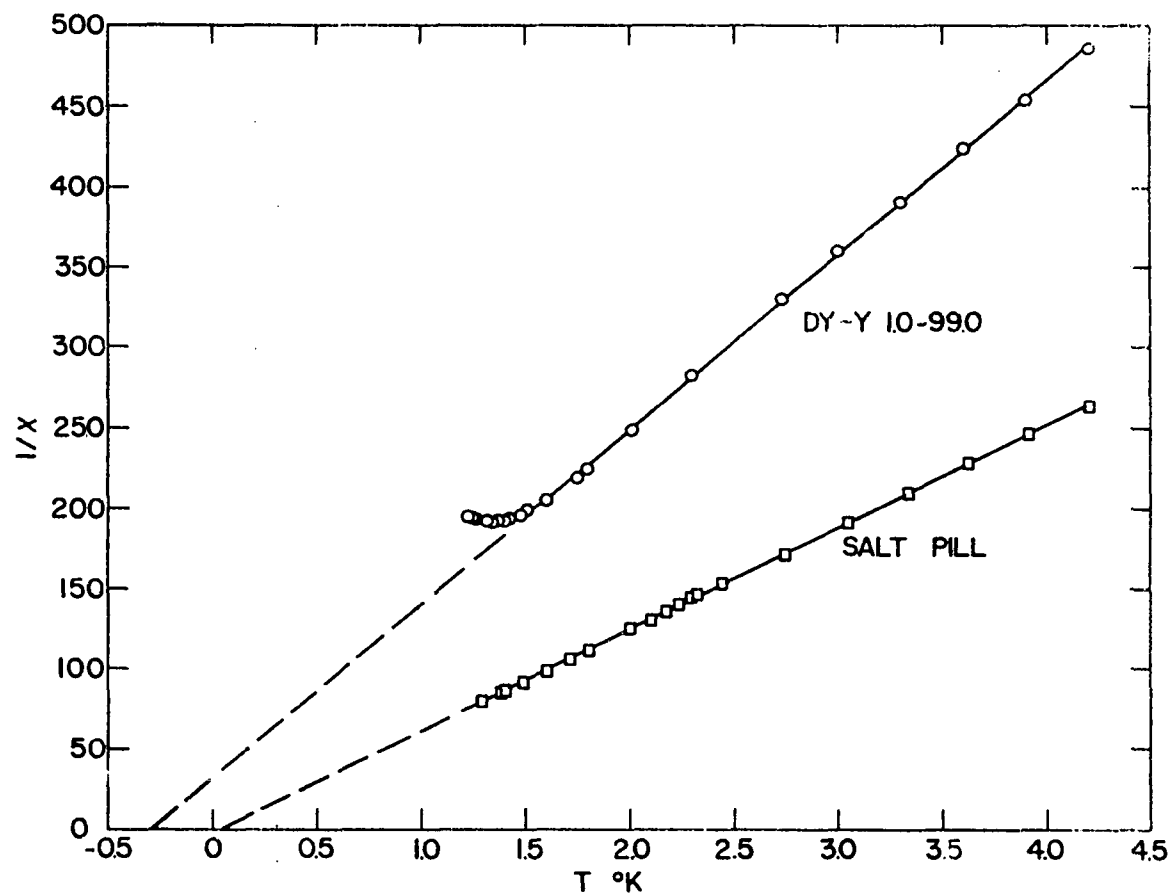
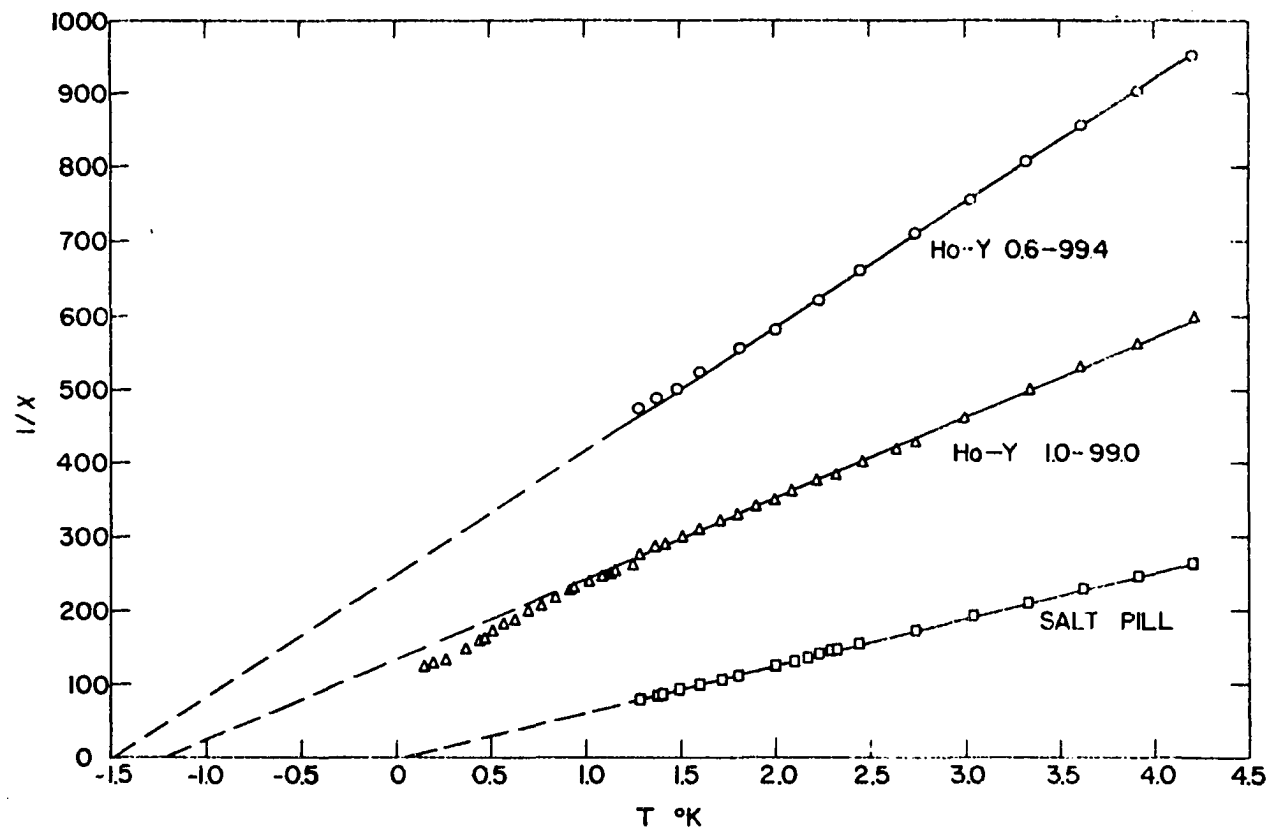


Figure 8. Inverse susceptibility versus temperature for the alloys Ho-Y 0.6-99.0 and Ho-Y 1.0-99.0. Data for a salt pill of iron ammonium alum are shown for comparison. See text.



lowest temperatures measured although there is a slight deviation from simple paramagnetism at the lowest temperatures. (Temperatures below 1.25 °K for the Ho-Y 1.0-99.0 alloy were obtained by cooling the sample with a demagnetized paramagnetic salt as described above.) The Curie constants obtained from the slopes of the straight portions of the plots are  $C = 0.0085$  for the 1.0 percent alloy and  $C = 0.0056$  for the 0.6 percent alloy. The intercepts with the temperature axis of the extrapolated straight lines are  $-1.23$  °K and  $-1.50$  °K, respectively. It should be noted that, although the Curie constants are approximately the same as the expected values, the actual susceptibility in this temperature region is roughly only half of what would be obtained if the alloys exhibited ideal paramagnetic behavior. The susceptibility of the 1.0 percent alloy at 1.5 °K is 0.0032 whereas the susceptibility of an ideal paramagnetic of the same Curie constant would be  $\chi = 0.0085/1.5$  or 0.0057. This difference is associated with the relatively large negative paramagnetic Curie temperature. It is interesting to note that there seems to be no evidence for a maximum in the susceptibility of the 1.0 percent alloy down to the lowest temperature of 0.15 °K. There is an increase in susceptibility at the lowest temperatures greater than would be obtained from simple paramagnetism as evidenced by the breaking away of the experimental data from the extrapolated straight line plot. There is no indication, however, that a maximum in the susceptibility is being approached.

The magnetic susceptibility of an alloy of 1.25 percent holmium with 98.75 percent ytterbium was measured. The sample was in the form of a cylinder  $5/8$  inch diameter by 1-1/2 inch long. The experimental

data are presented in the graph of Figure 9 along with data on a salt pill which are the same as those of Figure 7. From the graph it can be seen that there is no simple paramagnetism. Furthermore the susceptibility of this sample is extremely weak. This alloy has approximately the same number of holmium atoms per  $\text{cm}^3$  as does the alloy Ho-Y 1.0-99.0; yet at 1.5 °K the susceptibility of this Ho-Yb alloy is 0.00095 in comparison to 0.0032 for the holmium-yttrium alloy.

### Magnetization Measurements

The magnetization  $\sigma$ , in emu per gram, of a single crystal of Ho-Y 0.6-99.0 and a single crystal of Ho-Y 1.0-99.0 was measured as a function of magnetic field intensity at temperatures in the range 1.47 to 4.2 °K. Measurements were made with the a-axis parallel to the field at all temperatures and with the c-axis parallel to the field at one temperature. Large anisotropy was observed which caused the sample and sample rod to rotate from the c-axis position into the a-axis position at high fields and reduced temperatures.

The experimental data for the single crystal of Ho-Y 0.6-99.4 are plotted on the graph of Figure 10. Magnetization with the a-axis parallel to the field is plotted for temperatures of 1.47, 1.87, 3.01, and 4.20 °K. With the c-axis parallel to the field, only the data at 4.20 °K are available. For comparison purposes the dashed line of Figure 10 is a curve computed from Equation 10 for an ideal paramagnetic material at 1.47 °K of the same saturation magnetization.

It can be seen that the anisotropy in magnetization is very strong,

Figure 9. Inverse susceptibility versus temperature for the alloy Ho-Yb 1.25-98.75. Data for a salt pill of iron ammonium alum are shown for comparison. See text.

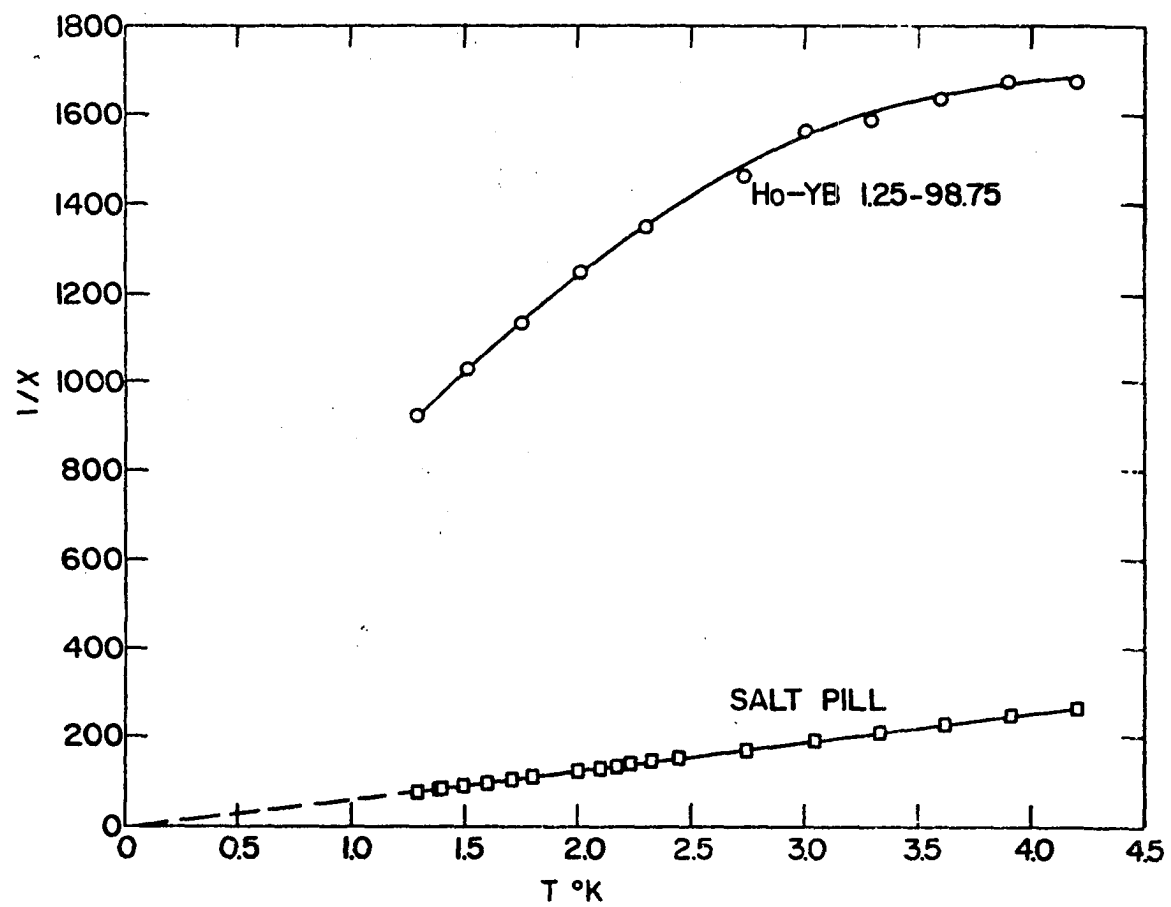
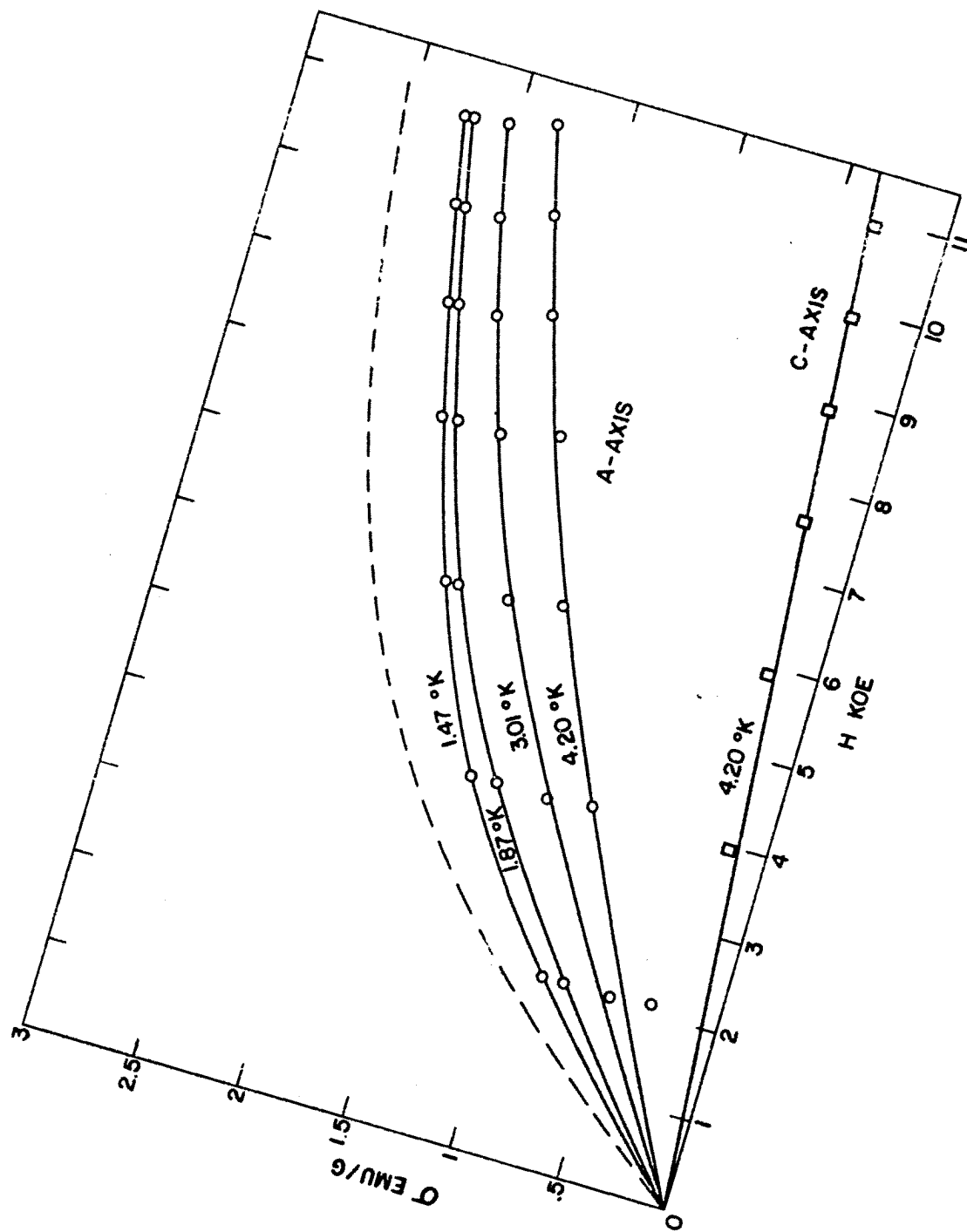




Figure 10.  $\sigma$  versus H for the single crystal of Ho-Y 0.6-99.4. The dashed curve represents the ideal paramagnetic behavior at 1.47 °K. See text.



with the a-axis magnetization fully 5 times the c-axis magnetization at 11 koe and 4.20 °K. The magnetization along the c-axis appears to vary linearly with the field up to the highest field, whereas the magnetization along the a-axis has the general behavior of the ideal magnetization but considerably reduced in magnitude from it. Isofield plots of  $\sigma$  versus T are shown in the left-hand graph of Figure 11. The plotted points are taken from the smoothed curves of Figure 10. The isofield plots are extrapolated to zero temperature in order to obtain values of  $\sigma_{H,0}$ . These values of  $\sigma_{H,0}$  are then plotted versus  $1/H$  and extrapolated to infinite field in order to determine the saturation magnetization  $\sigma_{\infty,0} = 2.9$  emu per gram. (It is this saturation value of 2.9 emu per gram which was used to normalize the dashed curve of Figure 10.)

The data for the single crystal of Ho-Y 1.0-99.0 are presented in a similar manner in the graphs of Figures 12-14. It can be seen that there is very strong anisotropy in the magnetization with the a-axis magnetization being more than 6 times the c-axis magnetization at 4.2 °K. The a-axis magnetization was found to fall considerably below the ideal magnetization at 1.49 °K. This is the same behavior as found with the alloy of 0.6 percent holmium. From the plot of  $\sigma_{H,0}$  versus  $1/H$  of Figure 13 it is seen that the extrapolated magnetization is  $\sigma_{\infty,0} = 4.8$  emu per gram. (It is this saturation value of 4.8 emu per gram which was used to normalize the dashed curve of Figure 12.) In Figure 14 are plotted data taken of  $\sigma$  versus H with the field increasing and decreasing. There is a noticeable hysteresis effect

Figure 11.  $\sigma$  versus T and  $\sigma_{H_2O}$  versus  $1/H$  for the single crystal of Ho-Y 0.6-99.0.

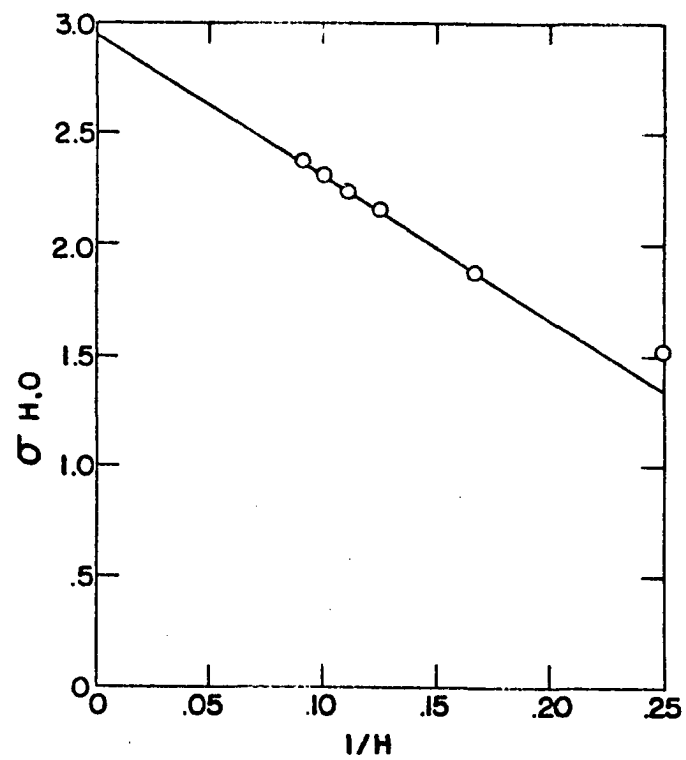
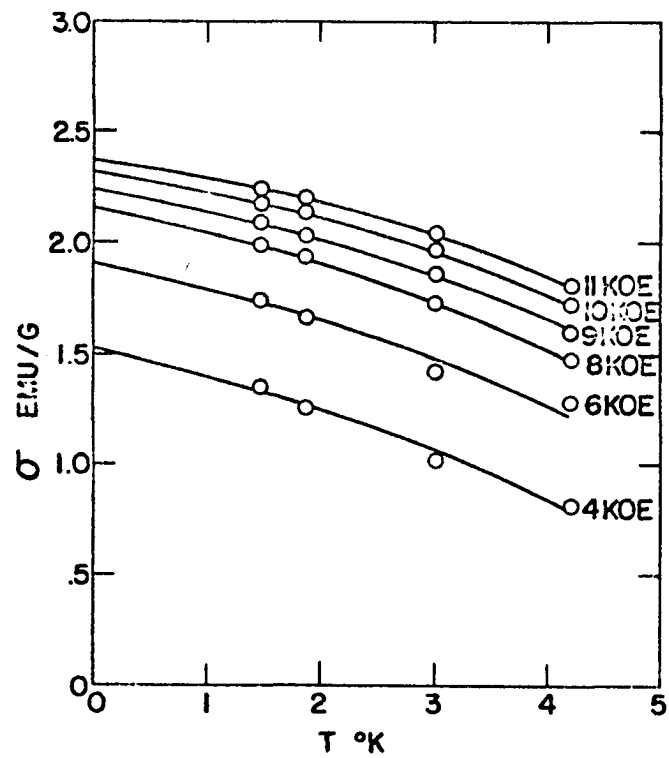


Figure 12.  $\sigma$  versus H for the single crystal of Ho-Y 1.0-99.0.  
The dashed curve represents the ideal paramagnetic  
behavior at 1.49 °K. See text.

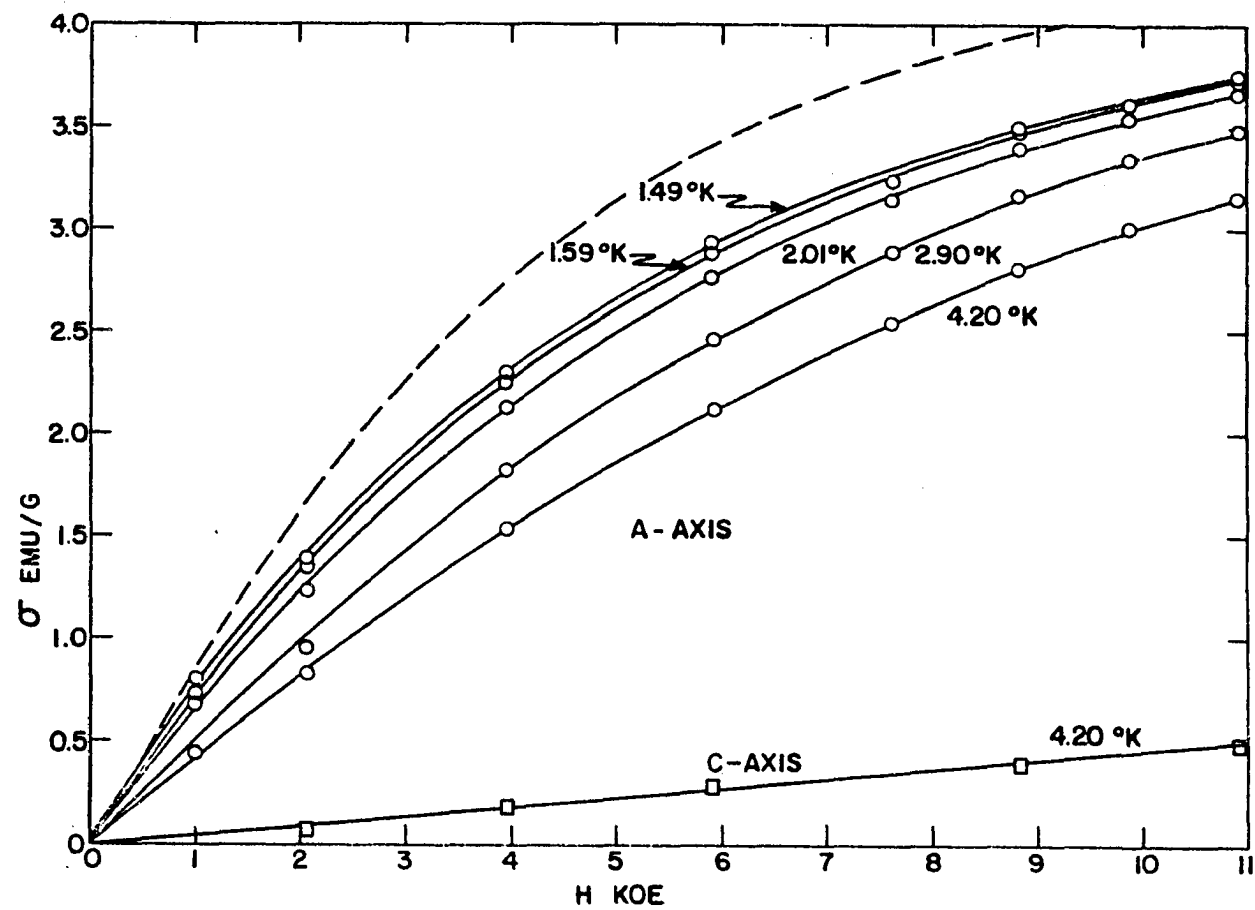


Figure 13.  $\sigma$  versus T and  $\sigma_{H,O}$  versus  $1/H$  for the single crystal  
of Ho-Y 1.0-99.0.



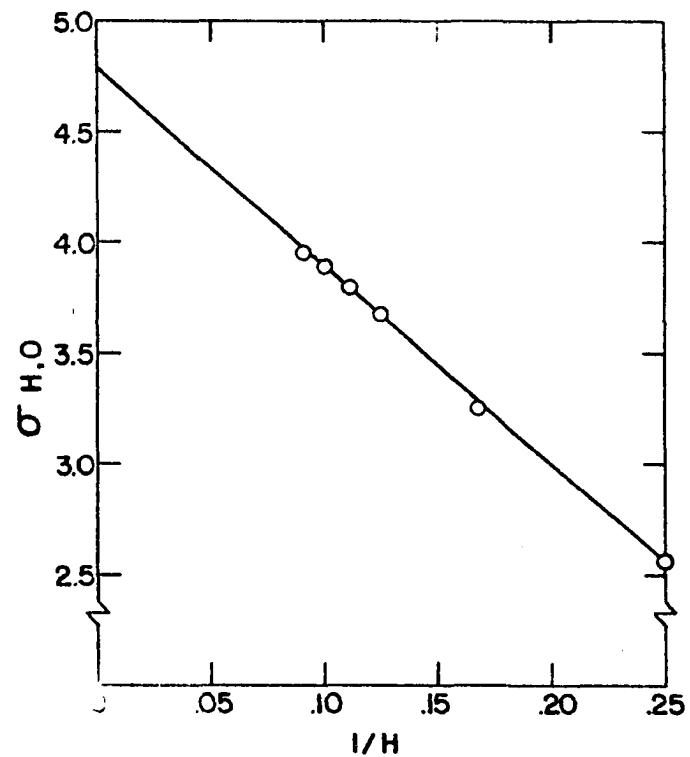
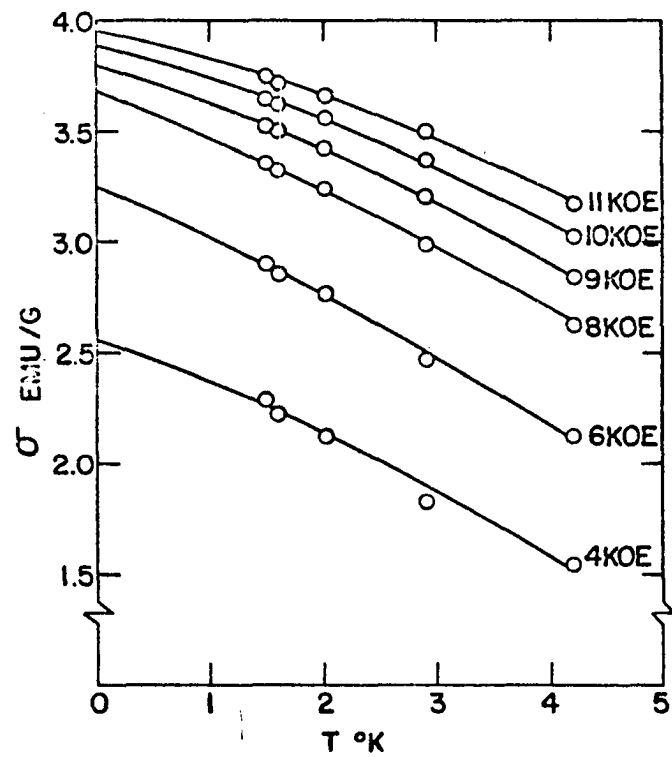
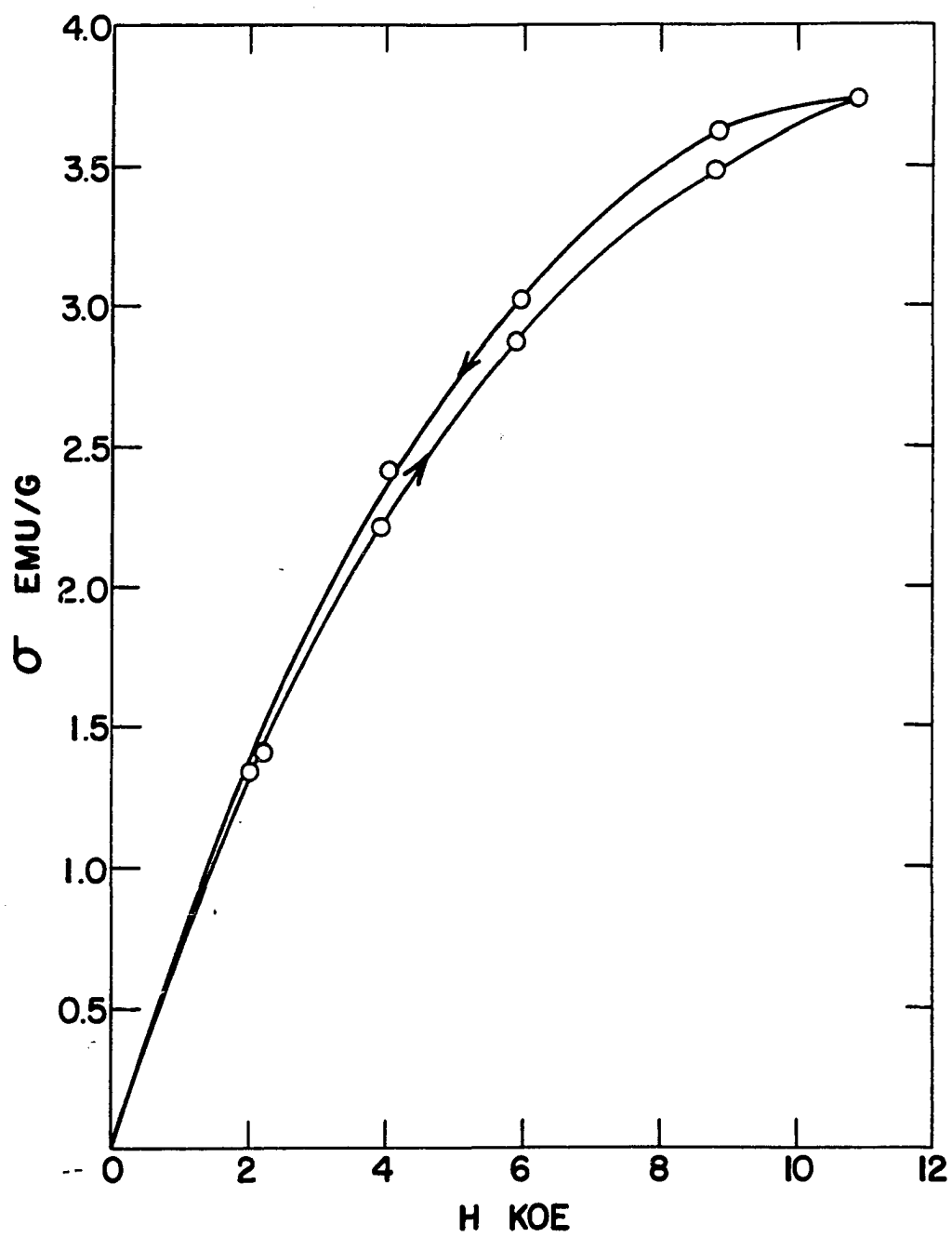


Figure 14.  $\sigma$  versus H at 1.58 °K for the single crystal of Ho-Y 1.Q-99.0 with field increasing and decreasing and with the a-axis parallel to the field.



indicating the presence of ferromagnetic inclusions in the sample.

#### Adiabatic Demagnetization Measurements

The materials examined by adiabatic demagnetization were those which exhibited paramagnetism down to the lowest measured temperatures. These were the following: Gd-Y 0.3-99.7, Ho-Y 0.6-99.4, and Ho-Y 1.0-99.0, the latter two both in polycrystalline and single crystal form.

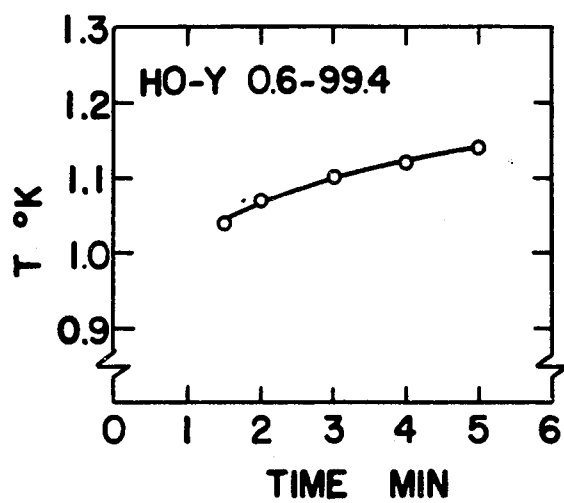
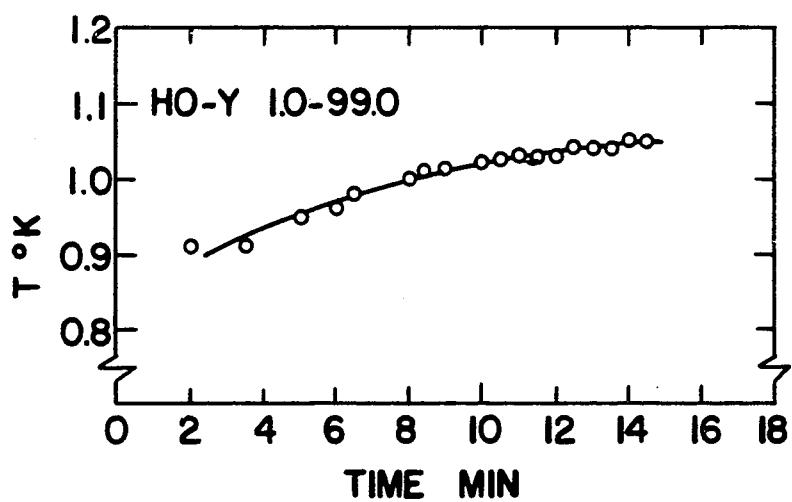
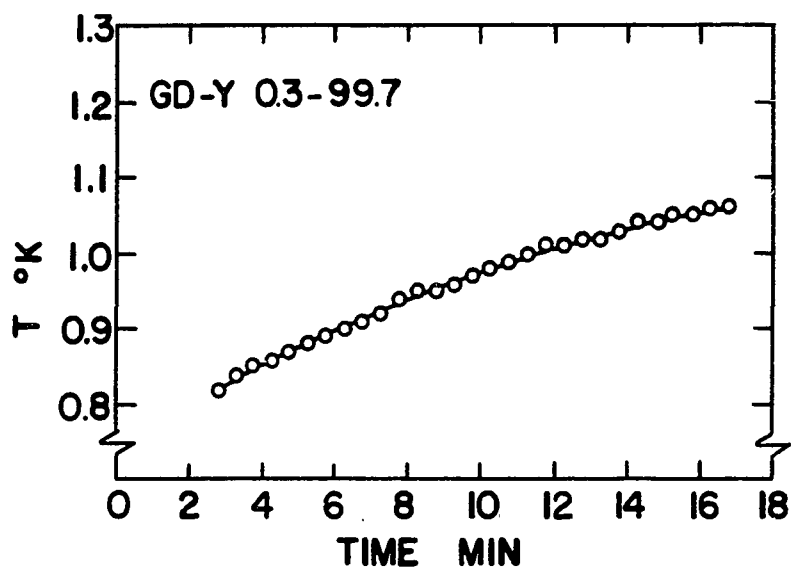
The Gd-Y 0.3-99.7 alloy was demagnetized from an initial temperature of 1.25 °K and a field of 10.6 koe. The lowest temperature recorded was 0.82 °K, and the temperature of the sample started to rise immediately as shown in the top graph of Figure 15. Since the demagnetization was carried out over a period of two minutes, the lowest temperature would have been reached two minutes after the start of the demagnetization. An extrapolation of the warming curve back to 2.0 minutes indicates that the lowest temperature actually obtained by the sample was probably 0.8 °K.

The rapid rise in temperature is most likely due to heat transfer from the walls of the sample tube via residual helium exchange gas. An estimate of this heat leak to the sample can be made by use of Knudsen's formula (61, p. 49) for heat transfer in the free molecular region.

$$q_t = 7275 p(T_1 - T_0)a / \sqrt{MT_0} \quad (21)$$

where  $q_t$  is the heat transfer in erg/sec cm<sup>2</sup>,  $p$  the pressure in dynes/cm<sup>2</sup>,  $T_1$  and  $T_0$  the warm and cold temperatures, respectively,  $a$

Figure 15. Warming curves after demagnetization of the alloys Gd-Y 0.3-99.7, Ho-Y 0.6-99.4, and Ho-Y 1.0-99.0. The abscissa denotes time in minutes after the start of the demagnetization.



the accommodation coefficient (equal to unity for "sticky" molecules), and  $M$  the gas molecular weight. With the sample of  $16 \text{ cm}^2$  area at  $1.0^\circ\text{K}$  and with the bath temperature at  $1.25^\circ\text{K}$  this gives a  $q_t$  of about 500 erg/min. Here  $a$  is taken as unity and  $p$  as  $5 \times 10^{-8} \text{ mm Hg}$ , which is the gauge pressure of about  $10^{-6} \text{ mm Hg}$  multiplied by the thermomolecular ratio  $1/\sqrt{300}$ . At  $1.0^\circ\text{K}$  the warming rate of the sample, as obtained from the graph of Figure 15 was  $.017^\circ\text{K/min}$ . The heat capacity at this temperature can be approximated by the electronic heat capacity of the yttrium in the sample. Jennings et al. (62) have shown the electronic heat capacity of yttrium to be

$$C_{el} = 85 \times 10^{-4} T \text{ joules/mole } ^\circ\text{K} \quad . \quad (22)$$

Using this value of heat capacity and the observed warming rate, the heat input to the sample of mass 22 g was found to be 350 erg/min at  $1.0^\circ\text{K}$ . From these calculations it can be seen that the heat leak due to residual exchange gas accounts for the rapid rise in temperature after demagnetization.

The alloy Ho-Y 1.0-99.0 was demagnetized from a field of 11.4 koe and a starting temperature of  $1.28^\circ\text{K}$ , and the Ho-Y 0.6-99.4 alloy from 11.4 koe and  $1.29^\circ\text{K}$ . The warming curves for these two samples are shown in the center and lower graphs of Figure 15, respectively. The lowest temperatures obtained were  $0.91^\circ\text{K}$  for the 1.0 percent alloy and  $1.04^\circ\text{K}$  for the 0.6 percent alloy. The warming rates are about the same as observed previously and can be accounted for by the presence of residual helium exchange gas as described above.

The single crystals of the holmium-yttrium alloys were demagnetized with the c-axis parallel to the field and with the a-axis parallel to the field. However the results obtained in the two cases were the same. The conclusion is that, because of the strong anisotropy in the magnetization and because of the flimsiness of the suspension in the sample chamber (see Figure 1), it is not possible to keep the sample from orienting itself with the a-axis parallel to the magnetic field. The results presented are those for demagnetization with the a-axis parallel to the field; no results are available for demagnetization with the c-axis parallel to the field.

The Ho-Y 0.6-99.4 alloy single crystal was demagnetized from an initial temperature of 1.25 °K and a magnetic field of 12.0 koe. The warming curve is plotted on the graph of Figure 16. The lowest temperature recorded was 0.83 °K. The warming rate agrees with that computed on the basis of residual exchange gas as described above. The slight change in warming rate at 37 minutes occurred at the same time that the voltage across the Wheatstone bridge was raised from .02 volt to .06 volt. The power input to the resistor with .02 volt across the bridge circuit is estimated to be about 2 ergs per minute which is only about one third of the heat input due to residual exchange gas. With the voltage raised to .06 volt, the energy dissipated in the carbon resistor becomes the dominant heat input - thus the increase in warming rate.

The Ho-Y 1.0-99.0 alloy single crystal was demagnetized from an initial temperature of 1.25 °K and a magnetic field of 11.4 koe. The warming curve is plotted on the graph of Figure 17. The lowest temperature recorded was 0.76 °K. The rate of warming agrees with that calculated on the basis of residual exchange gas, as before.



Figure 16. Warming curve after demagnetization of the alloy  
Ho-Y 0.6-99.4. The abscissa denotes time in  
minutes after the start of the demagnetization.

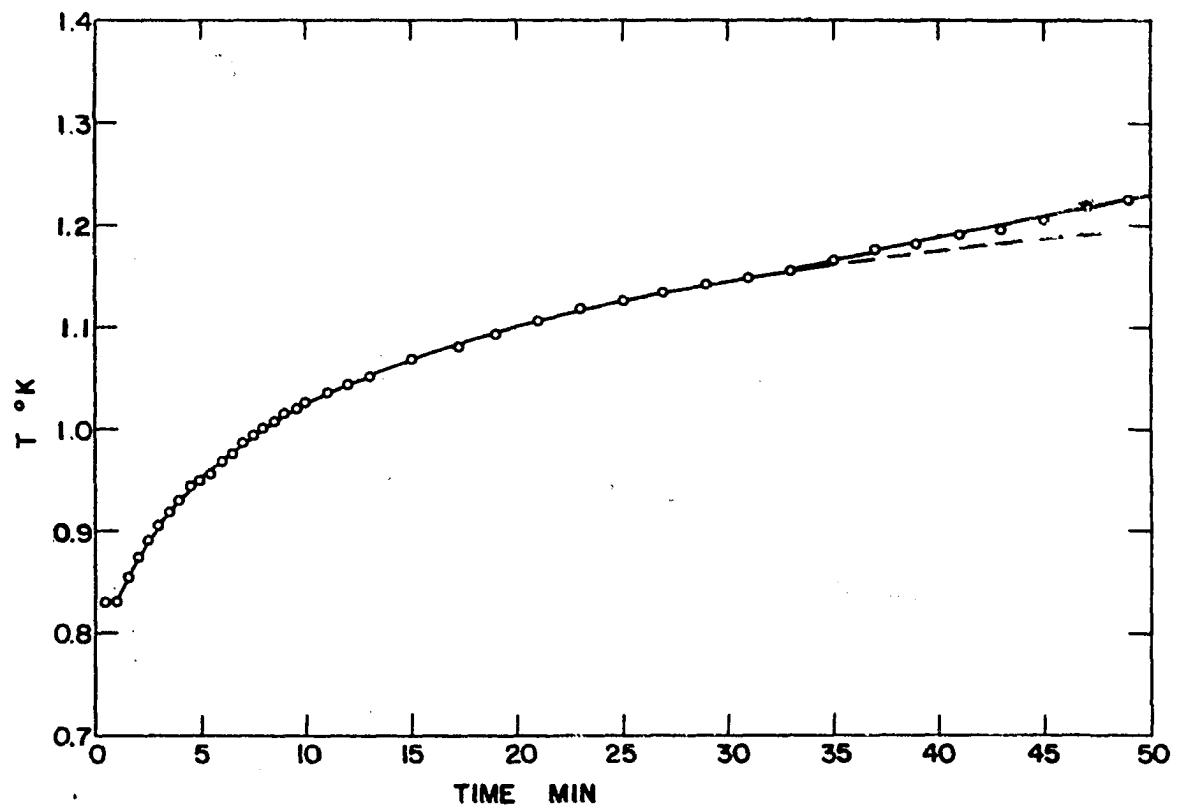
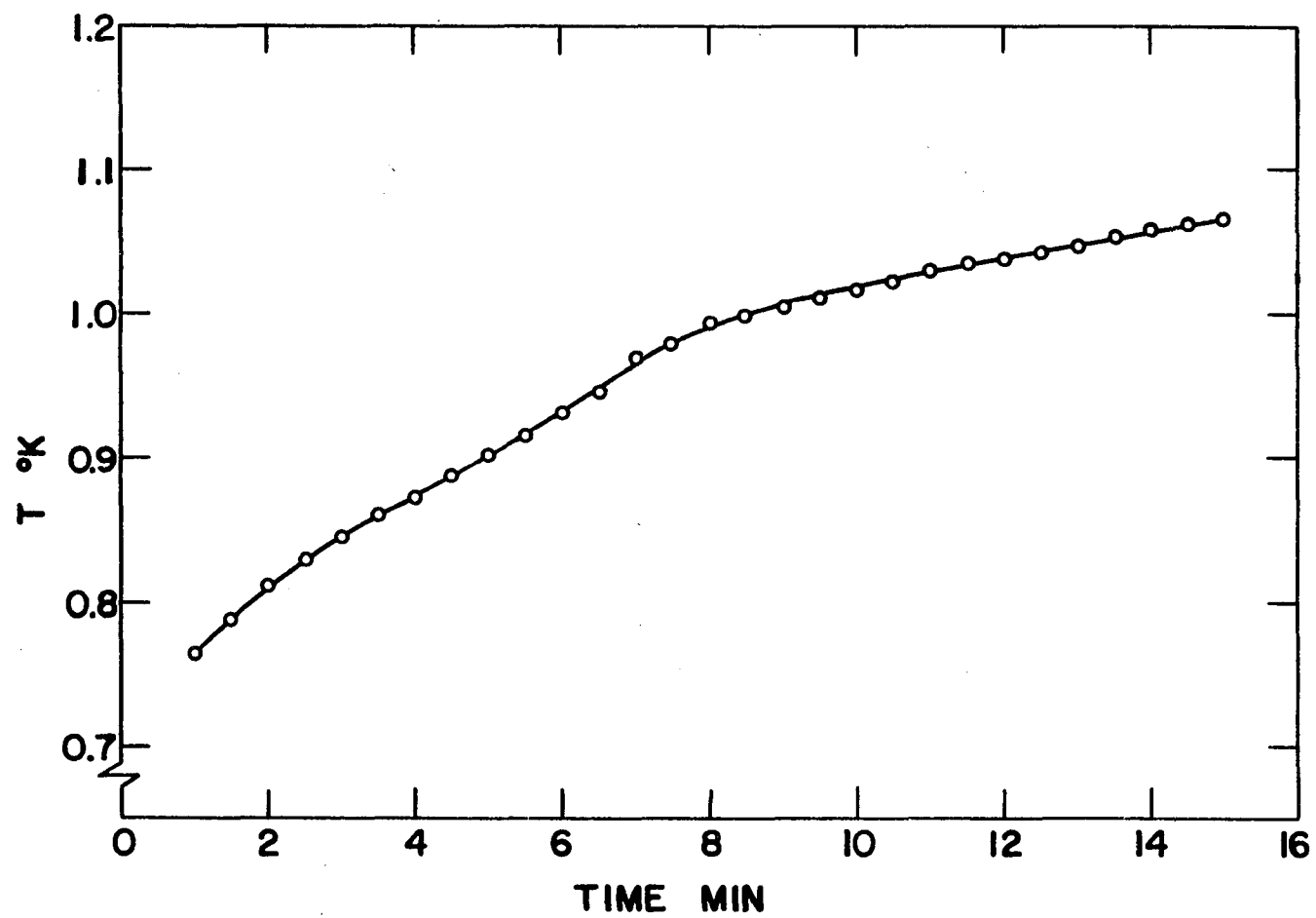


Figure 17. Warming curve after demagnetization of the alloy  
Ho-Y 1.0-99.0. The abscissa denotes time in  
minutes after the start of the demagnetization.



## DISCUSSION

A comparison between the observed Curie constants and those calculated using Equation 13 are shown in Table 7. It is apparent that

Table 7. Comparison of observed and calculated Curie constants for some alloys.

Alloy	C (observed)		C (calculated)
Gd-Y 0.3-99.7	.0023		.0012
Dy-Y 1.0-99.0	.0076		.0071
Ho-Y 0.6-99.4	.0056		.0043
Ho-Y 1.0-99.0	.0085		.0071

the observed Curie constants are somewhat larger than expected on the basis of the calculations. This can be explained, in part at least, by the presence of impurities in the samples. All the samples contained iron and nickel to the extent of about 0.02 percent by weight and oxygen in the following amounts: 0.13 weight percent in the gadolinium-yttrium alloys, 0.04 weight percent in the dysprosium-yttrium alloy, and 0.02 weight percent in the holmium-yttrium alloys. However, the contributions of these impurities to the Curie constant are small, being 0.0003, 0.0002, and 0.0001, respectively. From the hysteresis measurements on a holmium-yttrium single crystal it is apparent that there is a certain small

amount of ferromagnetism in this alloy. If this is due to ferromagnetic clustering of the solute metal, one would expect this to be present to some extent in all the alloys, representing a small departure from random dispersal of the solute atoms. This, in turn, would enhance the susceptibility and help account for the larger observed values. It should also be mentioned that Sato et al. (63) have pointed out that the  $1/\chi$  versus  $T$  curves for dilute alloys exhibit a slope which increases with temperature. Thus the Curie constant calculated from the slope of the curve would be overestimated at all but the high temperatures (near room temperature).

Magnetic transitions characteristic of antiferromagnetism were observed at 3.40 °K in the Gd-Y 1.0-99.0 alloy and at 1.34 °K for the Dy-Y 1.0-99.0 alloy. There is evidence of an approaching transition at 0.8 °K in the Gd-Y 0.3-99.7 alloy. No transition was observed in the holmium-yttrium alloys down to the lowest temperatures measured. Thoburn et al. (41) have determined the paramagnetic Curie temperatures and Néel points of gadolinium-yttrium alloys with large gadolinium concentrations. Between 60 percent and 25 percent gadolinium they find these two characteristic temperatures to be roughly the same. An extrapolation of their data to small gadolinium concentrations gives expected transition temperatures of 4 °K and 1 °K for the 1.0 percent and 0.3 percent alloys, respectively. These numbers are in reasonable agreement with the present results.

Néel (46) has suggested that the paramagnetic Curie points for the rare earths could be explained by assuming a spin-spin type of

interaction between magnetic ions so that

$$k\theta \propto S(S+1) \quad (23)$$

On the basis of this interaction one would expect the gadolinium alloy to have the highest magnetic transition temperature of the 1.0 percent alloys tested because it has the highest spin (refer to Table 1). More recently de Gennes (64) has suggested that correction to the spin-spin interaction should be made for spin-orbit coupling. He proposes that the Curie point should vary in the following manner:

$$k\theta \propto J(J+1)(g-1)^2 \quad (24)$$

Table 8 shows the observed magnetic transitions of the 1.0 percent alloys and calculated transitions using both Equations 23 and 24 normalized to

Table 8. Observed and calculated transition temperatures for 1.0 percent alloys of rare earth in yttrium.

Solute	$T_c$ °K (observed)	$T_c$ °K (calculated Equation 23)	$T_c$ °K (calculated Equation 24)
Gd	3.40	3.40	3.40
Dy	1.34	1.83	1.52
Ho	0.15	1.30	0.97

the transition of the gadolinium-yttrium alloy. It can be seen that the observed transition temperatures seem to vary more rapidly than predicted by either Equation 23 or Equation 24. A similar result was obtained by Bozorth et al. (65) who studied compounds of rare earth metals with the platinum metals.

Various proposals have been advanced in recent years which arrive at a method for determining the Curie point or the Neel temperature (depending whether the material goes ferro- or antiferromagnetic) in dilute magnetic systems. Owen et al. (35) using a molecular field treatment discuss a model of copper-manganese alloys in which the conduction electrons become magnetized by the ion cores. The conduction electrons are then considered as magnetizing other ions parallel to themselves, thus producing a cooperative effect leading to ferromagnetism at sufficiently low temperature. They predicted that the Curie point should vary linearly with  $S(S + 1)$  and with solute concentration. However their experimental results indicated that the dilute copper-manganese alloys became antiferromagnetic at low temperatures rather than ferromagnetic. Electron spin resonance measurements suggested that the coupling between ion cores and conduction electrons was ten or more times smaller than expected.

In a later paper Owen et al. (66) discuss a molecular field treatment of the copper-manganese alloy system with the manganese ions divided into two sublattices A and B in such a way that short range interactions give ferromagnetic coupling A-A, B-B, and antiferromagnetic coupling A-B. On this basis they show that the observed antiferromagnetic



ordering can be explained if the ferromagnetic indirect exchange via conduction electrons is much smaller than the short range antiferromagnetic exchange. They show that the Néel temperature should vary linearly with  $S(S + 1)$  and the concentration.

Pratt (67) discusses the theory of antiferromagnetic-ferromagnetic transitions in dilute magnetic alloys. He proposes that the direct exchange coupling between the conduction electrons and the  $d$  electrons of the ion cores can account for the observed antiferromagnetism in the dilute copper-manganese system and that it is comparable in magnitude to the antiferromagnetic coupling.

Statistical treatments of dilute magnetic systems have been given recently by Sato et al. (63), Brout (68), and Seiden (69). Sato et al. (63) point out that the molecular field treatment is quite inappropriate, even qualitatively, in the case of magnetically dilute solutions. This conclusion is based on the fact that a molecular field treatment predicts that the Curie point starts from zero concentration. Such a calculation takes into account interactions between both near and distant atoms with equal weight. Their statistical treatment arrives at a Curie point for the ferromagnetic transition which varies linearly with the strength of the interaction, but which is a linear function of the concentration only at high concentrations. A finite concentration such that  $c(z - 1) > 1$  ( $c$  = concentration,  $z$  = number of nearest neighbors) is required for the onset of ferromagnetism on this model. That is, the appearance of ferromagnetism coincides with the concentration for which the number of magnetic atoms is just greater than sufficient to make a linear chain in the crystal, on the average. A similar

conclusion is reached for a system with antiferromagnetic ordering.

Brout (68) has developed a statistical treatment, involving interactions among clusters of a finite number of particles, for a random ferromagnetic system. In the limit of extreme dilution and for nearest neighbor interactions only, the Curie point was calculated to be given by

$$\tanh (J/kT_c) = 1/xz \quad , \quad (25)$$

where  $z$  is the number of nearest neighbors,  $x$  the concentration, and  $J$  the interaction energy for nearest neighbor interactions. This predicts that ferromagnetism will not occur unless  $xz > 1$ , a conclusion roughly the same as that of Sato et al. (63).

Seiden (69), in a statistical treatment that considers ferromagnetic coupling in a random lattice, arrives at a Curie point which is proportional to  $S(S + 1)$  and to the concentration. No cutoff concentration was predicted which is in disagreement with the calculations of Sato et al. (63) and Brout (68).

The observed paramagnetic Curie temperatures  $\Theta$  and magnetic transition temperatures  $T_c$  are presented in Table 9 for comparison. A molecular field treatment predicts that  $\Theta = \pm T_c$  with the plus sign for ferromagnetism and minus sign for antiferromagnetism. The observed transitions are thought to be antiferromagnetic which should give a negative  $\Theta$ . This is observed for the Dy-Y 1.0-99.0 alloy; however, a positive  $\Theta$  is observed for the Gd-Y 0.3-99.7 alloy. This feature is not understood, nor is the fact that  $\Theta$  is larger for the 0.6 percent holmium-yttrium alloy than for the 1.0 percent alloy. It is expected

Table 9. Observed paramagnetic Curie temperature  $\Theta$  and observed magnetic transition temperature  $T_c$  for the alloys studied.

Alloy	$\Theta$	$T_c$
Gd-Y 0.3-99.7	+0.38	0.8 (?)
Gd-Y 1.0-99.0	(?)	3.40
Dy-Y 1.0-99.0	-0.28	1.34
Ho-Y 0.6-99.4	-1.50	1.25
Ho-Y 1.0-99.0	-1.18	0.15

that the magnetic transition temperature would be higher for higher solute concentrations, yet in this case the paramagnetic Curie temperature is found to be larger (in absolute value) for the weaker alloy. In this respect, Parks and Little (70) have found  $\Theta$  to be negative for two dilute alloys of dysprosium in yttrium and to be larger in absolute value for the more concentrated alloy.

The very strong anisotropy observed in the holmium-yttrium single crystals helps to explain part of the difficulty encountered in the adiabatic demagnetization of the polycrystalline holmium-yttrium alloys. After reaching a final temperature of 0.83 °K by demagnetization of the Gd-Y 0.3-99.7 alloy it was, at first, a mystery why the polycrystalline holmium-yttrium alloys could not be cooled even this much. (Since the holmium-yttrium alloys have considerably larger magnetic ion concentrations, and since holmium has a larger magneton number than gadolinium, it would be expected that considerably more entropy could be

removed during isothermal magnetization from the holmium-yttrium rather than the gadolinium-yttrium system.) Demagnetizations of the single crystals in the easy direction show that lower temperatures are obtained. This is a consequence of the greater degree of alignment obtained during the magnetization along the easy magnetic direction. However, there is, even yet, some property of these alloys which prevents them from being cooled to very low temperatures by adiabatic demagnetization. Entropy considerations (discussed below) will throw some light onto this problem.

The saturation magnetizations of the single crystal holmium-yttrium alloys from the extrapolated portions of the  $1/H$  plots of Figures 11 and 13 are presented in Table 10 along with the values expected as calculated from Equation 17. The observed values of  $\sigma_{a,0}$  are about 25 percent less than the predicted values in each case. It is interesting to note, however that the value of  $\sigma_{a,0}$  obtained for the 0.6 percent alloy is 60 percent of the value for the 1.0 percent alloy, as one would expect.

Table 10. Observed and predicted values of saturation magnetization for the single crystal holmium-yttrium alloys.

Alloy	$\sigma_{a,0}$ (observed)	$\sigma_{a,0}$ (predicted)
Ho-Y 0.6-99.4	2.9	3.78
Ho-Y 1.0-99.0	4.8	6.30

Bozorth et al. (65) find a similar depression of the saturation magnetization in holmium alloys with the platinum metals. They consider this to be a result of partial quenching of the orbital moments in holmium. However, no such quenching is apparent in pure holmium metal; the predicted saturation moment is truly obtained along a crystalline direction in the basal plane halfway between two  $a$ -axes<sup>a</sup>. Since the holmium ions in the holmium-yttrium alloys are in practically the same crystalline environment as they are in holmium metal, it is difficult to explain how quenching of orbital moments would occur in the alloys and not in the pure metal. Three other possible explanations can be offered for the smaller observed magnetizations: First, the  $1/H$  extrapolation to determine  $\sigma_{\infty,0}$  may not be appropriate, so that application of a strong enough field may produce the theoretical saturation. Second, it is possible that there is anisotropy in the basal plane of the alloys so that a larger magnetization may be found along a different crystalline direction. This latter point has not been investigated. Third, it is possible that part of the magnetic vector may be perpendicular to the basal plane such that those components along the  $a$ -axis are parallel aligned and those along the  $c$ -axis are antiparallel aligned. Thus the  $a$ -axis would behave like a ferromagnet and the  $c$ -axis like an anti-ferromagnet. Such behavior has been proposed for erbium (with the  $c$ -axis as the easy axis) by Koehler and Wollan (71) on the basis of neutron diffraction studies. Green (72) has found evidence to support this interpretation for erbium metal.

---

<sup>a</sup>Donald Strandburg and Sam Legvold, Ames, Iowa. Data obtained on magnetization of holmium single crystals. Private Communication. 1960.

In order to learn something concerning the demagnetization process with the single crystals, entropy calculations have been made from the magnetization curves as presented on the graphs of  $\sigma$  versus  $T$  at constant  $H$  (see Figures 11 and 13). The value of  $\left(\frac{\partial \sigma}{\partial T}\right)_H$  at 1.25 °K was determined for various  $H$ , then the entropy extraction during the isothermal magnetization was computed from Equation 3. The entropy extraction expected for an ideal paramagnetic during isothermal magnetization was computed from the following relation:

$$\frac{\Delta S}{R} = \log(2J + 1) - \frac{\partial}{\partial T} \left[ T \log \sum_{m=-J}^J \exp(-m g \mu_B H / kT) \right]_H. \quad (26)$$

The numbers obtained from Equation 26 were multiplied by 0.01 for the 1.0 percent alloy and 0.006 for the 0.6 percent alloy. The electronic entropy change from the initial to the final temperature during demagnetization was calculated for each alloy from Equation 22. These numbers are presented in Table 11. It is immediately apparent that these alloys

Table 11. Entropy changes encountered in magnetization and demagnetization of the single crystal alloys.

Alloy	$\frac{\Delta S}{R}$ (ideal)	$\frac{\Delta S}{R}$ (actual)	$\frac{\Delta S_{el}}{R}$
Ho-Y 0.6-99.4	.009	.0016	.0004
Ho-Y 1.0-99.0	.015	.0020	.0005

behave far from ideally. The very low observed entropy extraction is a consequence of the poor temperature variation of magnetization at constant field. From this it would seem that interactions between magnetic ions are not negligible at 1.25 °K even though the magnetic susceptibility data do not deviate from the Curie-Weiss law down to the lowest measured temperatures. This is corroborated by the fact that the total entropy extraction is considerably larger than the change in electronic entropy which occurs during the cooling. Since the lattice entropy is negligible at these temperatures (62), there must be a contribution to heat capacity from magnetic ion interactions.

In conclusion it can be seen that the alloy systems investigated are not useful alloys for adiabatic demagnetization. The magnetic behavior of the alloys investigated are far from ideal at temperatures even as high as 1.25 °K. Quite recently, Parks and Little (70) have reported magnetic cooling experiments with thorium-rare earth alloys. At a starting temperature of 0.73 °K and a magnetic field of 8 koe they have succeeded in cooling alloys of various concentrations. They reached 0.1 °K with a 1.90 atomic percent dysprosium in thorium alloy. They have reported entropy versus temperature data for the various alloys. However, they have computed the entropy from Equation 26 with a small correction for the electronic entropy of thorium. Such a calculation explicitly assumes that magnetic interactions are negligible at the magnetization temperature (0.73 °K in this case). Their plots of entropy versus temperature indicate that this is definitely not the case since the slope of  $S$  versus  $T$  is too steep at 0.73 °K. Thus their entropy calculations are open to question. It would appear that the alloys

which they have studied exhibit the same peculiar properties as those studied in this research; namely, that the magnetization curves fall considerably below the ideal behavior of a paramagnetic substance.

The program which has been undertaken leaves some questions unanswered which present areas for further study. No definite conclusions were reached concerning the effect of the number of conduction electrons on the Curie point of a dilute alloy. The holmium-ytterbium system was only weakly paramagnetic down to 1.25 °K, whereas the europium-ytterbium system was apparently ferromagnetic at 4.2 °K. This latter system would be especially interesting to study, particularly because of the present uncertain status concerning the magnetic properties of pure europium.



## SUMMARY

The magnetic susceptibility of some dilute alloys of rare earth metals in yttrium and ytterbium has been measured for temperatures below 4.2 °K. Alloys of gadolinium in yttrium showed a maximum in the susceptibility characteristic of an antiferromagnetic transition at 3.4 °K for 1 percent gadolinium and probably near 0.8 °K for 0.3 percent gadolinium. A similar anomaly was observed at 1.34 °K for 1 percent dysprosium in yttrium. Alloys of holmium in yttrium of 0.6 and 1.0 percent holmium showed no such anomaly down to 1.25 °K and 0.15 °K, respectively. An alloy of 1.25 percent holmium in ytterbium was only weakly paramagnetic down to 1.25 °K whereas an 0.4 percent europium in ytterbium alloy was apparently ferromagnetic at 4.2 °K.

Magnetization measurements on single crystals of 0.6 percent and 1.0 percent holmium in yttrium alloys were made in the temperature range 1.47 °K to 4.20 °K and in magnetic fields up to 11 koe. Anisotropy was observed with the magnetization in the direction of the a-axis being more than 5 times that in the direction of the c-axis. The extrapolated saturation magnetizations in the a-direction were 2.9 and 4.8 emu/g for the 0.6 and 1.0 percent alloys, respectively, compared with 3.8 and 6.3 emu/g, respectively, expected for ideal paramagnetic behavior.

Adiabatic demagnetizations were performed on the 0.3 percent gadolinium-yttrium alloy and the single crystals of 0.6 and 1.0 percent holmium in yttrium alloy from a field of about 11 koe at 1.25 °K. The

lowest temperatures achieved were 0.83 °K, 0.81 °K, and 0.76 °K, respectively. Entropy calculations based on the magnetization measurements of the single crystals indicate that the entropy extracted during magnetization is only about 15 percent of that expected from an ideal paramagnetic. The conclusion is drawn that there are rather large magnetic interactions between solute ions at temperatures as high as 1.25 °K even though susceptibility measurements would not indicate this.

## LITERATURE CITED

1. Kammerlingh Onnes, H., Chem.-Ztg. 32, 901 (1908).
2. Keesom, W. H., Proc. Roy. Soc. (Amsterdam) 35, 136 (1932).
3. Blaisse, B. S., Cooke, A. H., and Hull, R. A., Physica 6, 231 (1939).
4. Debye, P., Ann. Physik 81, 1154 (1926).
5. Giauque, W. F., J. Am. Chem. Soc. 49, 1864 (1927).
6. Giauque, W. F. and McDougall, D. P., Phys. Rev. 43, 768 (1933).
7. De Haas, W. J., Wiersma, E. C., and Kramers, H. A., Physica 1, 1 (1934).
8. Kurti, N. and Simon, F., Nature 133, 907 (1934).
9. Ambler, E. and Hudson, R. P., Repts. Progr. in Phys. 18, 251 (1955).
10. Kurti, N., Rollin, B. V. and Simon, F., Physica 3, 266 (1936).
11. Mendoza, E. and Thomas, J. G., Phil. Mag. 42, 291 (1951).
12. Meyer, H., J. Phys. Chem. Solids 9, 296 (1959).
13. Miedema, A. R., Postma, H., Van der Vlugt, N. J., and Steenland, M. J., Physica 25, 501 (1959).
14. Daunt, J. G. and Heer, C. V., Phys. Rev. 76, 985 (1949).
15. Heer, C. V., Barnes, C. B., and Daunt, J. G., Phys. Rev. 91, 412 (1953).
16. Heer, C. V., Barnes, C. B., and Daunt, J. G., Rev. Sci. Instr. 25, 1088 (1954).
17. Mendelssohn, K. and Moore, J. R., Nature 133, 413 (1934).
18. Mendelssohn, K., Daunt, J. G., and Pontius, R. B., Proc. Intern. Congr. Refrig. 7th Congr. (The Hague-Amsterdam) 1, 445 (1936).
19. Mendelssohn, K., Nature 169, 336 (1952).
20. Daunt, J. G. and Mendelssohn, K., Nature 143, 719 (1939).

21. Kapitza, P., J. Phys. (U.S.S.R.) 5, 59 (1941).
22. Landau, L., J. Phys. (U.S.S.R.) 5, 71 (1941).
23. Simon, F., Physica 16, 753 (1950).
24. Sydoriak, S. G., Grilly, E. R., and Hammel, E. F., Phys. Rev. 75, 303 (1949).
25. Zinov'eva, K. N., Soviet Phys. - JETP 2, 774 (1956).
26. Sydoriak, S. G. and Roberts, T. R., Phys. Rev. 106, 175 (1957).
27. Seidel, G. and Keesom, P. H., Rev. Sci. Instr. 29, 606 (1958).
28. Sommers, H. S., Jr., Keller, W. E. and Dash, J. G., Phys. Rev. 92, 1345 (1953).
29. Brewer, D. F., Nature 185, 349 (1960).
30. Gorter, C. J., Physik. Z. 35, 923 (1934).
31. Kurti, N. and Simon, F., Proc. Roy. Soc. (London) A 149, 152 (1935).
32. Rollin, B. V. and Hatton, J., Phys. Rev. 74, 346 (1948).
33. Kurti, N., Robinson, F. N. H., Simon, F. E., and Spohr, D. A., Nature 178, 450 (1956).
34. Hodben, M. V. and Kurti, N., Phil. Mag. 4, 1092 (1959).
35. Owen, J. Browne, M., Knight, W. D., and Kittel, C., Phys. Rev. 102, 1501 (1956).
36. Hedgcock, F. T., Phys. Rev. 104, 1564 (1956).
37. Schmitt, R. W. and Jacobs, I. S., J. Phys. Chem. Solids 3, 324 (1957).
38. Jacobs, I. S. and Schmitt, R. W., Phys. Rev. 113, 459 (1959).
39. Bates, L. F. and Newmann, M. M., Proc. Phys. Soc. (London) 72, 345 (1958).
40. Matthias, B. T., Suhl, H., and Corenzwit, E., Phys. Rev. Letters 1, 92 (1958).
41. Thoburn, W. C., Legvold, S., and Spedding, F. H., Phys. Rev. 110, 1298 (1958).
42. Van Vleck, J. H., Am. J. Phys. 18, 495 (1950).

43. Hodgman, C. D., Weast, R. C., and Selby, S. M., eds. Handbook of chemistry and physics. 39th ed. Cleveland, Ohio, Chemical Rubber Publishing Company. 1957 .
44. Spedding, F. H., Legvold, S., Daane, A. H., and Jennings, L. D. Some physical properties of the rare earth metals. In Gorter, C. J., ed. Progress in low temperature physics. Vol. 2, pp. 368-394, Amsterdam, North-Holland Publishing Company, 1957.
45. Klemm, W. and Bommer, H., Z. anorg. u. allgem. Chem. 231, 138 (1937).
46. Neel, L., Compt. rend. 206, 49 (1938).
47. Hall, P. M., Legvold, S., and Spedding, F. H., Phys. Rev. 116, 1446 (1959).
48. Maxwell, J. C. A treatise on electricity and magnetism. 3rd ed., Oxford, Clarendon Press. 1904.
49. Schmid, L. P. and Smart, J. S., U. S. Naval Ordnance Report No. 3640 (1954).
50. Spedding, F. H. and Daane, A. H., J. Am. Chem. Soc. 74, 2783 (1952).
51. Spedding, F. H., Daane, A. H., Carlson, O. N., Schmidt, F. H., Haeffling, J. A., Haberman, C. E., and Wakefield, G. F. Preparation of yttrium metal. In Banks, C. V., Carlson, O. N., Daane, A. H., Fassel, V. A., Fisher, R. W., Olson, E. H., Powell, J. E., and Spedding, F. H. Studies on the preparation, properties and analysis of high purity yttrium oxide and yttrium metal at the Ames Laboratory. pp. 51-96. U. S. Atomic Energy Commission Report IS-1 Iowa State University . July, 1959.
52. Greninger, A. B., Trans. Am. Inst. Mining, Met. Engrs. 117, 61 (1935).
53. Henry, W. E. and Dolecek, R. L., Rev. Sci. Instr. 21, 496 (1950).
54. Brickwedde, F. G., van Dijk, H., Durieux, M., Clement, J. R., and Logan, J. K., J. Research Natl. Bur. Standards 64A, 1 (1960).
55. De Klerk, D. and Hudson, R. P., J. Research Natl. Bur. Standards 53, 173 (1954).
56. Cooke, A. H., Meyer, H., and Wolf, W. P., Proc. Roy. Soc. (London) A 233, 536 (1956).
57. Elliott, J. F. The ferromagnetic properties of the rare earth metals. Unpublished Ph. D. Thesis. Ames, Iowa, Iowa State University of Science and Technology Library, 1953.

58. Thoburn, W. C. Magnetic properties of Gd-La and Gd-Y alloys. Unpublished Ph.D. Thesis. Ames, Iowa, Iowa State University of Science and Technology Library, 1956.
59. Nicol, J. and Soller, T., Bull. Am. Phys. Soc. 2, 63 (1957).
60. Clement, J. R., Quinell, E. H., Steele, M. C., Hein, R. A., and Dolecek, R. L., Rev. Sci. Instr. 24, 545 (1953).
61. Knudsen, M. The kinetic theory of gases. London, Methuen and Company, Ltd. (1934).
62. Jennings, L. D., Miller, R., and Spedding, F. H. The lattice heat capacity of the rare earths. The heat capacities of yttrium and lutetium from 15-350 °K. Institute for Atomic Research and Department of Chemistry, Iowa State University, Ames, Iowa. Mimeo. Report. ca. 1960 .
63. Sato, H., Arrott, A., and Kikuchi, R., J. Phys. Chem. Solids 10, 19 (1959).
64. De Gennes, P. G., Compt. rend. 247, 1836 (1958).
65. Bozorth, R. M., Matthias, B. T., Suhl, H., Corenzwit, E., and Davis, D. D., Phys. Rev. 115, 1595 (1959).
66. Owen, J., Browne, M. E., Arp, V., and Kip, A. F., J. Phys. Chem. Solids 2, 85 (1957).
67. Pratt, G. W., Jr., Phys. Rev. 108, 1233 (1957).
68. Brout, R., Phys. Rev. 115, 824 (1959).
69. Seiden, J., Compt. rend. 250, 485 (1960).
70. Parks, R. D. and Little, W. A., Magnetic cooling with thorium-dysprosium alloys. VIIIth International Conference on Low Temperature Physics, Toronto, 1960. Official Programme, 354-356, 1960.
71. Koehler, W. C. and Wollan, E. O., Phys. Rev. 97, 1177 (1955).
72. Green, R. W. Electrical and magnetic properties of erbium single crystals. Unpublished Ph. D. Thesis. Ames, Iowa, Iowa State University of Science and Technology Library, 1960.

## ACKNOWLEDGMENTS

It is a pleasure for the author to express his appreciation to Dr. Sam Legvold who suggested this investigation and guided it through to completion. The author also wishes to thank Dr. C. A. Swenson for many helpful suggestions. The author is also indebted to Dr. F. H. Spedding for supplying the pure metals, to Mr. F. A. Schmidt for preparing the arc-melted alloys and to Mr. C. E. Habermann for preparing the cast alloys. He is further appreciative of the helpfulness of the members of the Low Temperature Laboratory under the supervision of Mr. W. Sylvester for their assistance in the design and building of apparatus. Finally, the author wishes to thank Mr. J. Beaver who helped in taking most of the data.